UNIVERSITY OF SOUTHERN QUEENSLAND

The Impact of Photocatalytic TiO_2 on Permeable Concrete Mix Designs and its Application for the Degradation of Organic Pollutants in Water

A Dissertation submitted by

Jason. R. Bolt DAppSc (Chemistry), BSc (Chemistry)

For the award of

MASTERS OF ENGINEERING RESEARCH

2013

Abstract

The project examines the influence of the addition of photocatalytic titanium dioxide (TiO_2) to permeable concrete with respect to percentage voids, permeability, mix designs, void connectivity and the degradation of organic pollutants within the fluid stream. It was unclear what effect the addition of TiO_2 would have on the properties of permeable concrete as little or no research had been reported in this area of study. It was necessary to design and produce "standard" permeable concrete mixes to establish a baseline to measure the impact of adding TiO_2. The percentage of voids present in permeable concrete produced was determined and compared by applying two different methods, apparent density (standard test), and an image analysis approach. This allowed determination of any effect that the photocatalytic titanium dioxide had on the hydraulic and mechanical properties of the permeable concrete. The effectiveness of photocatalytic titanium dioxide permeable concrete was analysed under laboratory conditions for the degradation of naphthalene, a poly-aromatic hydrocarbon in a fluid load. The process was to expose permeable concrete samples containing 5, 10 and 15 percentage addition of titanium dioxide to ultra violet light irradiation to compare the relative breakdown of pollutant (as represented by naphthalene). The research has shown, TiO_2 significantly reduced the workability of the permeable concrete and helped to ensure increased void space. The increased surface area of permeable concrete, with the addition of TiO_2 significantly improved the degradation rate of naphthalene compared to traditional concrete pavement.

Key words:

Permeable Concrete, Pores, Permeability, Void, Photocatalyts, TiO_2, Degradation, Water

Certification of Dissertation

I certify that the ideas, experimental work, results, analyses, software and conclusions reported in this dissertation are entirely my own effort, except where otherwise acknowledged. I also certify that the work is original and has not been previously submitted for any other award, except where otherwise acknowledged.

_____ _____

Jason Bolt, Candidate Date

ENDORSEMENT

_____ _____

Associate Professor Yan Zhuge, Principal Supervisor Date

_____ _____

Professor Frank Bullen, Associate Supervisor Date

Acknowledgments

The author would like to thank the following for their support and encouragement; The University of Southern Queensland, BASF Australia, Associate Professor Yan Zhuge, Professor Frank Bullen and Rachel Bolt. Thank you, also to the companies who supported this research with time, materials and access to your laboratories ; Premix Concrete, Direct Mix Concrete, Boral Asphalt, Boral Concrete, LabSA, Adelaide Brighton Cement, & Degussa.

Table of Contents

1.0 Introduction

This project investigated the incorporation of photocatalytic titanium dioxide (TiO_2) in permeable concrete for the degradation of organic pollutants. Investigations included the comparison of a standard concrete mix to permeable concrete mixes, both incorporating varying percentages of photocatalytic TiO_2, and comparing their breakdown of a polyaromatic hydrocarbon (PAH). The permeable concrete was cast in large simulated pavement moulds, where non-standard laboratory compaction methods were applied to simulate field permeable pavements. A single PAH was chosen to represent organic pollutants found in urban waste waters, such as motor ways and footpaths. Naphthalene was analysed during the trials, as research had shown that it was frequently found at urban sites and because it has reduced toxicity compared to other PAHs.

The research aimed to test whether permeable concrete is superior for the breakdown of organic pollutants by photocatalytic degradation, the hypothesis being that permeable concrete, having an increased surface area compared to normal concrete, would be superior. It is the intention of this research to benefit the concrete industry by contributing to the body of knowledge that already exists in this area, and to potentially apply it to practical uses in the future.

1.1 Background Research

Water Security, including the availability of potable waters is an international issue. This is particularly important in Australia, which has some of the "driest" cities in the world. For example, every year around 230,000 megalitres of stormwater and treated effluent is pumped out to sea in South Australia, which is greater than Adelaide's annual consumption of water. South Australia is the driest state in Australia, which has a Mediterranean climate with cold winters and dry, hot summers, with an average rain fall of only 236mm per year. Urban catchments such as roads, footpaths and car parks are all major catchments for runoff water. These waters contain heavy metals and hydrocarbons that either go straight out to sea or to water treatment plants, and are then pumped out to sea. Permeable concrete can allow this runoff water to filter through pores in the pavement, breaking down harmful pollutants and chemicals with the aid of aerobic bacteria, and then allow filtered water into the groundwater. Therefore the applications for permeable concrete pavements could play a vital role in our urban environment and waste water management systems for such cities.

The application of photocatalytic detoxification of polluted water has been discussed in Scientific Literature since 1976 (Carey *et al* 1976). Since then, some of the major applications have been the degradation of organic pollutants in water, the purification of air and the photocatalytic anti-bacterial effect in so-called "self cleaning" building materials (Cheen & Poon 2009). Photocatalytic oxidization takes place on the surface of the photcatalyst under ultra violet (UV) light. A photon of light is absorbed by the TiO_2, which starts a chemical reaction by producing an electron hole pair. This electron hole pair can then further produce hydroxyl radicals.

Two phenomena occur as a result of these factors; one is the photo-induced redox reaction of absorbed substances, the other is the photo-induced super-hydrophilicity (Chen & Poon 2009). The photo induced redox reaction is able to break down organic substances where the super-hyrdohilicity cleans away the substances from the surface.

Titanium dioxide (TiO_2) is the most commonly used photocatalyst in the construction industry (Chen & Poon 2009, Husken, Hunger & Brouwers 2009, Sanchez & Sobolev 2010). Traditionally TiO_2 has been used as a white pigment for building materials such as concrete, tiles and mortars. Research has shown that the modified cement containing TiO_2 is an effective means of breaking down organic pollutants (Chen & Poon 2009, Sanchez & Sobolev, 2010).

Permeable concrete has an increased surface area compared to normal concrete pavement. Adding TiO_2 to permeable concrete would be more effective, but there has been no research performed in this area.

1.2 Research Objective

The primary objective of this research is to gain an extensive understanding of the relationship between void ratio, effective void ratio and permeability in permeable concrete and the effect that TiO_2 has on the mechanical and hydraulic properties. This was investigated by comparing various techniques currently being used for void measurement and permeability measurement.

The second objective is to establish the effectiveness of the addition of TiO_2 to permeable concrete for the degradation of organic water pollutants. Varying quantities of TiO_2 and various void ratios were trialled to investigate optimum mix design for degradation. The objectives were investigated through a series of laboratory trial mixes, where the trial samples were subjected to mechanical and hydraulic testing.

Finally, the samples were tested for water quality improvements, through controlled laboratory analysis, which tested the degradation rate of a simulated road runoff, containing the pollutant naphthalene.

1.3 Structure of the Thesis

A literature review has been conducted to examine previous studies into the porosity of permeable concrete and photocatalytic construction materials, which is presented in Chapter 2 of this thesis. Following this, Chapter 3 summarises all the materials used in the experiments. Chapter 4 details the methodologies applied in testing the parameters of the mechanical and hydraulic properties of the photocatalytic permeable concrete. The mechanical and hydraulic results are discussed in Chapter 5. Chapter 6 reviews the degradation of naphthalene results. A conclusion on the effectiveness of photocatalytic permeable concrete for the degradation of organic compounds and recommendations for future research is discussed Chapter 7 and Chapter 8.

2.0 Literature Review

Permeable concrete is also known as Pervious Concrete, Porous Concrete, and No Fines Concrete (Kevern *et al*, 2005; Lain, Zhuge & Beecham, 2011; Park *et al* 2010; Scholz & Grabowiecki, 2006; Zhuge 2007). Although it is a low-strength structural concrete, which is made from cementitious materials and aggregates similar to those of traditional concrete pavement, permeable concrete has an interconnected void network. This is created by the reduction of fine material in the mix that allows water to be able to pass through the concrete. Permeable concrete has only been used in Australia for the last decade and has shown to be a positive sustainable solution to urban waste water management (Zhuge 2007).

2.1 Structural Performance of Permeable Concrete

The continuous voids that are formed in permeable concrete, through their unique design and compaction methods, also greatly reduce its compressive strength (Chindaprasirt *et al* 2006; Crouch, Pitt & Hewitt 2007; Kevern *et al* 2005; Wang *et al* 2006). Crouch, Pitt & Hewitt (2007), investigated the effects of increasing the quantity of aggregate, which resulted in higher effective voids as well as a decrease in compressive strength. It was concluded that the strength loss was due to a decrease in paste available for aggregate bonding, which lowered compressive strength. Similarly, Chindaprasirt *et al* (2006) examined the fractured surfaces after compression and found that the high void ratio concrete factures were almost entirely paste. Kevern *et al* (2005) noted that loss in strength by increasing the void ratio was linear. This was also seen in the findings of Wang *et al* (2006), where compressive strength results were effectively halved when doubling the void ratio.

Studies have shown that by using single sized small aggregates, low water cement ratios (0.2 – 0.35), and a sound knowledge of cement paste rheology, a permeable concrete with a void ratio between 15 – 25% can still achieve desired strengths (Chindaprasirt *et al* 2006; Crouch, Pitt & Hewitt 2007; Kevern *et al* 2005). Crouch, Pitt & Hewitt (2007) found that using smaller single sized aggregate resulted in higher compressive strength but similar void content, compared to using larger graded aggregate.

Chindaprasirt *et al*'s (2006) findings showed that cement paste with a water cement ratio ranging from 0.15 – 0.25, with a high flow 150-230mm (super-plasticised), produced permeable concrete with a void ratio between 15-25% and compressive strength of 15-38 MPa. When the aggregate size was increased, Kevern *et al* (2005) observed that the samples failed at the contact between the cement paste and aggregate.

Using small quantities of clean sand (approximately 7%) in the mix design also increased the compressive strength of the concrete but did not greatly reduce the void ratio (Kevern *et al* 2005; Wang *et al* 2006). Kevern *et al* (2005) presented results which showed that a 7% addition of fine sand resulted in a void ratio reduction of 6.3% and 8.3%, with a strength improvement of 57% and 84% respectively.

Furthermore, Wang *et al* (2006) found that incorporating 7% sand into the mix design reduced the void ratio by 10% down to 18.5%, but achieved a strength increase of 68%. However it does appear that Kevern and Wang's 7% addition of sand to improve the compressive strength by 20% had not been trialled extensively. Although strength increases were observed, varying percentages of sand additions do not appear to have been trialled.

The effect of aggregate on compressive strength of permeable concrete was investigated by Lian and Zhuge (2010). They found that dolomite was the best aggregate among all other used aggregates in Australia to make porous concrete. They also found the water content was one of the paramount factors for the compressive strength of porous concrete.

2.2 Void Ratio Measurement

Generally, the void content of permeable concrete is measured by a standard test, where the difference in weight between dry and wet cylinders are compared, then divided by the volume. However, some researchers have shown that this common test method is not effective in measuring porosity (Marlof *et al* 2004; Neithalath, Weiss & Olek 2009; Safiuddin & Hearn 2005). Safiuddin & Hearn (2005) compared three American Standard Test Method (ASTM) permeability methods and adapted them for measuring porosity.
They found that the standard void measurement test was not effective in measuring dead end pores. Their findings concluded that vacuum saturation ASTM C 1202 was more efficient in measuring dead end pores. Marlof *et al.* (2004) used an epoxy to penetrate the pores of the concrete. After cutting the cylinder (figure 2.1), image analysis was used to determine the actual void ratio. Neithalath, Weiss & Olek (2009) applied the same method. Their findings showed a considerable increase in void ratio compared to the standard method.

Figure 2.1 Cylinders after being cut for image analysis (Source Marlof *et al* 2004)

Further comparisons of the standard measurement test, vacuum saturation ASTM 1202 and the epoxy image analysis test are still required to determine which method is most applicable for permeable concrete.

Mathematical factors still need to be derived for the standard void ratio analysis, so that they can be applied when designing permeable concrete. This will assist engineers when designing future permeable concrete pavements and more accurate test methods.

2.3 Permeability and Pore Connectivity

Networks in permeable concrete differ quite considerably to normal concrete, standard methods for measuring hydraulic conductivity (permeability) cannot be applied. It is generally considered that the Falling Head method is best practice (Kevern *et al* 2005; Luck *et al* 2009; Wang *et al* 2006).

Kevern *et al* (2005) applied the Falling Head method (figure 2.2) and found that the reduction in void ratio reduced the permeability considerably. Similarly, Wang *et al* (2006) found that the permeability increased exponentially with the concrete void content, when applying the Falling Head method. Studies presented by Fortes, Merighi & Bandeira (2009), also showed that an increase in permeability meant a loss in strength and an increase in void ratio.

The coefficient of permeability (k) is determined by the following equation when Falling Head method is used:

$$k = \frac{aL}{At} \ln\left(\frac{h_1}{h_2}\right) \tag{2.1}$$

k= coefficient of permeability, cm/s
a = cross sectional area of stand pipe
A= Cross sectional area of specimen
L = length of sample
t= time in seconds from h1 to h2
h_1 = initial water level
h_2 = final water level

Figure 2.2 Measurement of permeability (Image from Kevern *et al*, 2005)

The flow rate of water through permeable concrete for the Falling Head Method ranges from 0.2cm/s to greater than 1cm/s for normal designed permeable concrete. However, if the network system of voids does not interconnect to allow the water to travel through the concrete, this rate is greatly reduced (Haselbach, Valavala & Montes 2006).

The Constant Head Method is another method commonly used for measuring the permeability of permeable concrete. Although this method is similar to the Falling Head Method, it differs in that water is continually passed through the sample and collected over a given time to measure the permeability. Recently, research by Lian, Zhuge & Beecham (2010) compared the Falling Head Method to Constant Head Method. Their studies showed that both test methods produced a similar trend. The Constant Head results were significantly lower than the Falling Head Method.

One method for determining the pore connectivity has been developed by Neithalath *et al* (2009), which measured the electrical conductivity of the concrete in a NaCl solution and by applying a modified parallel model. By using the conductivity method they effectively showed that permeability is not a function of porosity or pore size, but rather, of pore connectivity. They also found that the electrical impedance measurements which were used to obtain pore connectivity were directly related to the acoustic absorption of the material.

Although the common practice for measuring permeability is the falling head method, this method only measures the permeability. It does not measure pore connectivity. Further research is required for a simple method to determine pore connectivity.

2.4 Pollutant Removal in Permeable Concrete

Permeable concrete is not only good for allowing water to re-enter the water table, but is effective in purifying water, by reducing pollutants such as nitrogen and phosphorus (Gilbert 2006; Kwiatkowski *et al* 2007; Luck *et al* 2008; Luck *et al* 2009; Parks & Tia 2003).
Parks & Tia (2003) produced permeable concrete samples and then exposed them to bio-film, to which aquatic microbes could attach themselves.

They found that increasing the surface area of the concrete, through reducing the size of the aggregate and increasing the void content of the concrete, was effective in the removal of phosphorus and nitrogen. They also concluded that permeable concrete could be effectively used for the continuous purification of water.

Luck *et al* (2008) found that permeable concrete was effective in separating solid/liquid waste in effluent water and in causing a significant reduction in total nitrogen, soluble phosphorus, and total phosphorus. It was thought that the soluble phosphorus was reduced by reacting with the calcium and magnesium which was present in the concrete. This allowed the phosphorous to precipitate as calcium or magnesium phosphate.

Further studies were carried out by Luck *et al* (2009) who investigated the use of permeable concrete for filtering cow manure.

It was observed that permeable concrete reduced the impact on the environment by reducing the amount of nutrients such as total Nitrogen, total Phosphorus, Ammonium, Nitrate ion (tN,tP,NH_4^+, NO_3^-) and pathogens, through filtering and storing.

Gilbert (2006) investigated asphalt, crushed limestone and permeable pavers used in driveways and compared the pollutant run off. Their findings showed that permeable pavers had the lowest concentration of pollutants; Total Suspended Solids, Ammonia, Nitrate ion, Total Kjeldahl Nitrogen, Total Phosphorus, Copper, Lead, and Zink (TSS, NH_3, NO_3^-, TKN, tP, Cu, Pb, Zn) present in the runoff water. In 2007, Kwiatkowski *et al* (2007) conducted field tests on a permeable concrete infiltration basin system at Villanova University and concluded that permeable concrete was an effective means of controlling stormwater without having a negative effect on groundwater.

In the above studies permeable concrete has been shown to be effective in breaking down the total nitrogen and phosphorus pollutants. However, there appears to be a gap in the research of the use of permeable concrete to break down organic pollutants in road runoff with the addition of a photocatalyst.

2.5 Application of Photocatalytic Titanium Dioxide to Building Materials.

Road runoff waters are exposed to vehicle pollution. The main pollutants are polycyclic aromatic hydrocarbons (PAH), mineral oils, and heavy metals (Schipper *et al* 2007). Schipper *et al* (2007) conducted field trials for 13 months, examining road runoff and vehicle spray on two motorways. Their findings showed that pollutants affected the top soils, ground water and surface water, and that the concentration of contaminants over time exceeded standard limits.

Over the past decade there has been significant research and development in the area of photocatalysts (Shi *et al* 2009). One of the major applications has been photo-induced redox reaction and super-hydrophilic conversion of TiO_2 for its degradation of organic pollutants (Bahnemann 2004; Chen & Poon 2009; Chen & Poon 2011; Shi *et al* 2009; Toada 2008).

Chen & Poon's (2009) paper on photocatalytic construction materials discussed the application of titanium dioxide (TiO_2) being added to construction material products such as tiles, glass, concrete, and paints. It was found that the products could be used for water and air purification, self cleaning, and self-disinfecting.

TiO_2 has been used in the construction industry traditionally as a white pigment. Although it is approximately 10 times more expensive than cement, it is a similar cost to coloured concrete, per metre cube. Chen & Poon's (2009) research detailed how photocatalytic TiO_2 affects organic pollutants and oxides such as NO, NO_2 and SO_2 by the photo-induced redox reaction.

Shi *et al* (2009) immobilized TiO_2 onto the surface of coal flyash (CFA), by three different methods; sol-gel, ambient hydrolysis and hybrid slurry procedure. Although not all methods were equally effective, all proved to be effective in the photocatalytic depigmentation and mineralization of methyl orange solution.

Laboratory studies carried out by Husken, Hunger and Brouwers (2009) showed that photocatalytic concretes were an effective solution for air purification, by successfully breaking down nitric oxide (NO) to nitrogen dioxide (NO_2) and thereafter to nitrate (NO_3^-). The process was described as a two-stage reaction on the surface of the photocatalyst:

$$NO + OH^{\cdot} \rightarrow NO_2 + H^+ \quad (2.2)$$

$$NO_2 + OH^{\cdot} \rightarrow NO_3^- H^+ \quad (2.3)$$

Husken, Hunger and Brouwers' (2009) research also found that increasing the surface area of the TiO_2 had a greater effect on the degradation rate of pollutants, than increasing the quantity of TiO_2. Recommendations for further study were made by Husken, Hunger and Brouwers (2009), which included increasing the surface layers by having a porous structure, which would increase the surface area of the TiO_2 and hence, increase the degradation rate of pollutants.

Research presented by Toada (2008) discussed the incorporation of TiO_2 to silica-gel. 420 grams of photocatalytic silica-gel was exposed to UV lamps in a photocatalytic system. Excreted waste water was treated for 240 minutes in the system and the excreted waste water appeared clear, odourless and deemed suitable for recycled usage.

There appears to be very little research performed on real scale projects. However, Bahnenmann (2004) discussed the practical application of photocatalysts being used in pilot plants, where results had been successful in the photocatalytic detoxification of polluted water, and the reaction mechanisms which took place.

Lackhoff *et al* (2003) analysed three modified TiO_2 and a ZnO photocatalytic powders and blended them with cement, to compare their effectiveness for the degradation of pollutants on building surfaces. The results showed that ZnO caused strong retardation of the hydration process and had significantly less photocatalytic activity than the TiO_2. A blend of 70% anatase and 30% rutile TiO_2 crystal formation proved to be the most efficient. It was noted that the addition of TiO_2 (70/30) increased the relative strength by 20%, due to the pozzolanic activity of the TiO_2.

2.6 Summary

The literature review explains that there are various methods for measuring porosity and permeability of permeable concrete. As the connecting voids contribute to the permeability of the concrete, it is the aim of this research to determine which method for measuring effective voids and permeability is most effective for photocatalytic permeable concrete (PPC) and hopefully to establish a relationship between void ratio and permeability for PPC.

According to the literature review, permeable concrete is quite effective in reducing inorganic pollutants from entering the groundwater via stormwater and polluted water.
However, most road runoff waters contain organic pollutants such as Poly-aromatic Hydrocarbons (PAH). Significant research in recent years has shown that TiO_2 modified concrete products are capable of breaking down organic pollutants in water.

From the literature review, it appears that there is little known about incorporating TiO_2 into permeable concrete for the degradation of organic pollutants in water. Similarly, there is little about what impact TiO_2 will have on the mix design properties.
For example, whether the addition of TiO_2 reduces the workability and makes it impossible to place the concrete on-site or whether it significantly reduces the mechanical properties. In either of these two examples the application of Photocatalytic Permeable Concrete is therefore unknown.

The major emphasis of this study is to examine the optimum addition of TiO_2 to permeable concrete, compared to the effective void ratio for organic pollutant breakdown under ultra violet light irradiation.

3.0 Materials

3.1 Concrete Trials Materials

All materials used for the concrete trial mixes are listed below in Table 3.1

Table 3.1. Overview of materials used in concrete trials

Material	*Manufacturer*	*Type*	*Size*
Cement	Adelaide Brighton Cement	General Portland	NA
Fly ash	Flinders Power	Coarse Fly ash	NA
Aggregate	Penrice	Limestone	20mm (Graded)
Aggregate	Penrice	Limestone	10mm (Graded)
Aggregate (Sand)	Clinton	Quartz sand	<4.75mm
TiO_2	Degussa	Aeroxide P25	<150 um

3.1.1 Cement

The cement used in this study was kindly donated by Adelaide Brighton Cement Limited (ABCL). The Cement samples were supplied in 20Kg bags. Representative samples of cement were supplied. The bags were sealed in plastic bags to ensure no degredation would occur before use. The cement type used for all the trials was type GB Premium Cement, which complies with AS 3972 -2010 General Purpose and Blended Cements. Type GB Premium Cement also contains 20 percent fly ash which complies with AS 3582.1 – 1998 Supplementary Cementitious Material for use with Portland and Blended Cement – Part 1: Flyash. Table 3.2 and Table 3.3 are the chemical composition and physical properties of the cement.

Table 3.2. X-Ray fluorescent spectroscopy results of ABCL GB cement

Oxides	*SiO_2*	*Al_2O_3*	*Fe_2O_3*	*CaO*	*SO_3*	*Na_2O*	*K_2O*	*MgO*	*Mn_2O_3*	*P_2O_5*	*CO_2*
%	27.15	9.52	3.15	52.01	1.87	0.69	0.52	1.60	0.08	0.18	1.40

Table 3.3. Loss on ignition and surface area results of ABCL GB cement

Loss on ignition	*Fineness index*
2.25 %	396 Kg/m^2

Loss of Ignition and fineness index are important characteristics of the cement properties. Loss of ignition is the percentage of carbon present in the cement after it has been burnt at high temperatures to remove organics. The fineness index is the surface area of the cement, this can have an effect on the workability and set times of the concrete.

3.1.2 Sand

The sand used in this study was supplied by Clinton Sands. The sand was sourced from Port Clinton, South Australia and was chosen because of its consistency and low clay content. Clinton Concrete sand complies with AS 2758.1 – 2006.

The characteristics are listed in the table below. A grading of the sand can be seen in Table 3.4 and Figure 3.1, which was produced in Excel by the researcher and compares to the standard. A 5 ton stock pile was stored, covered and used for the project. This was to prevent contamination of the material and reduce any material variances during the trials. The stock pile was turned over with machinery and a sample pad was made, prior to each trial.

Table 3.4 Characteristics of Clinton Sand

	Percentage passing by weight							*Silt*	*S.S.D*	*Water Absorption*
Sieve (mm)	*4.75*	*2.36*	*1.18*	*0.600*	*0.300*	*0.150*	*0.075*	*%*	*T/m³*	*%*
%	100.0	97.8	87.2	64.9	26.7	7.2	3.2	10.9	2.62	0.4

Note: SSD = Surface Saturated Dry

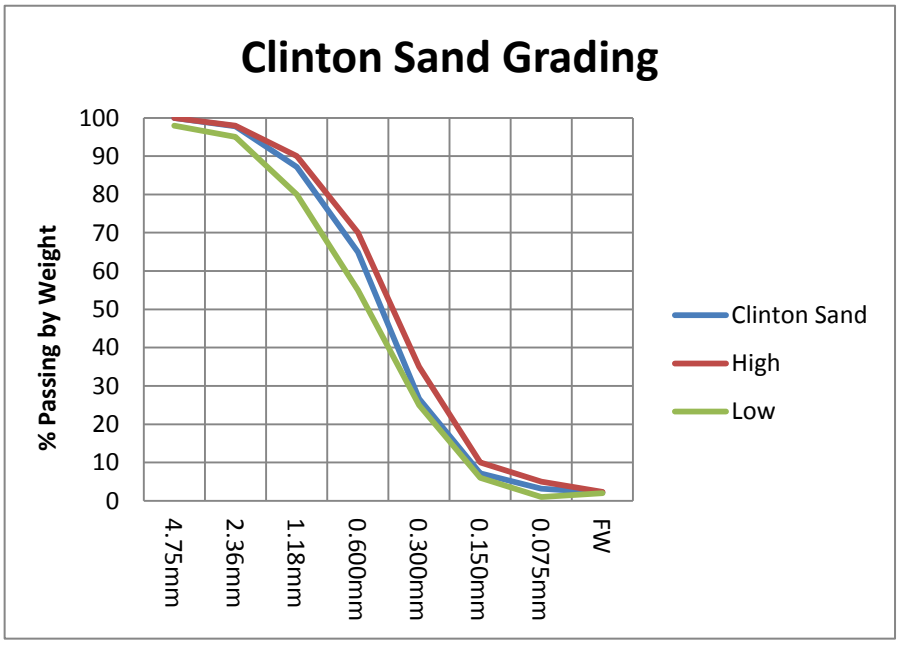

Figure 3.1 Grading of Clinton Sand Compared to Australian Standard

3.1.3 Aggregate

The stone used in all trials was Penrice 10-7mm concrete aggregate. This aggregate was kindly donated by Premix Concrete. The Penrice material is sourced from Angaston, South Australia, and is a calcareous aggregate. The 10-7mm concrete aggregate complies with AS 2758.1 - 2006 and the characteristics are listed in the table below. A grading of the aggregate compared to the standard was created by the author and is shown in Figure 3.2. Like the sand, a 5 ton stock-pile was stored and covered for the project, with representative samples taken from the stock-pile for the trial mixes.

Table 3.5 Characteristics of Penrice 10mm aggregate

	Percentage passing by weight								*LA*	*Wet*	*WD*	*S.S.D*
Sieve (mm)	*19.0*	*16.0*	*13.2*	*9.5*	*6.7*	*4.75*	*2.36*	*1.18*	*Value*	*kN*	*%*	*T/m³*
%	100.0	100.0	100.0	70.7	17.0	3.5	2.4	2.4	41.6	71.9	15.2	2.68

Note: LA = Loss Angeles Abrasion Testing
Wet = Aggregate Wet Strength
WD = Wet Dry Strength Variation
S.S.D = Surface Saturated Dry

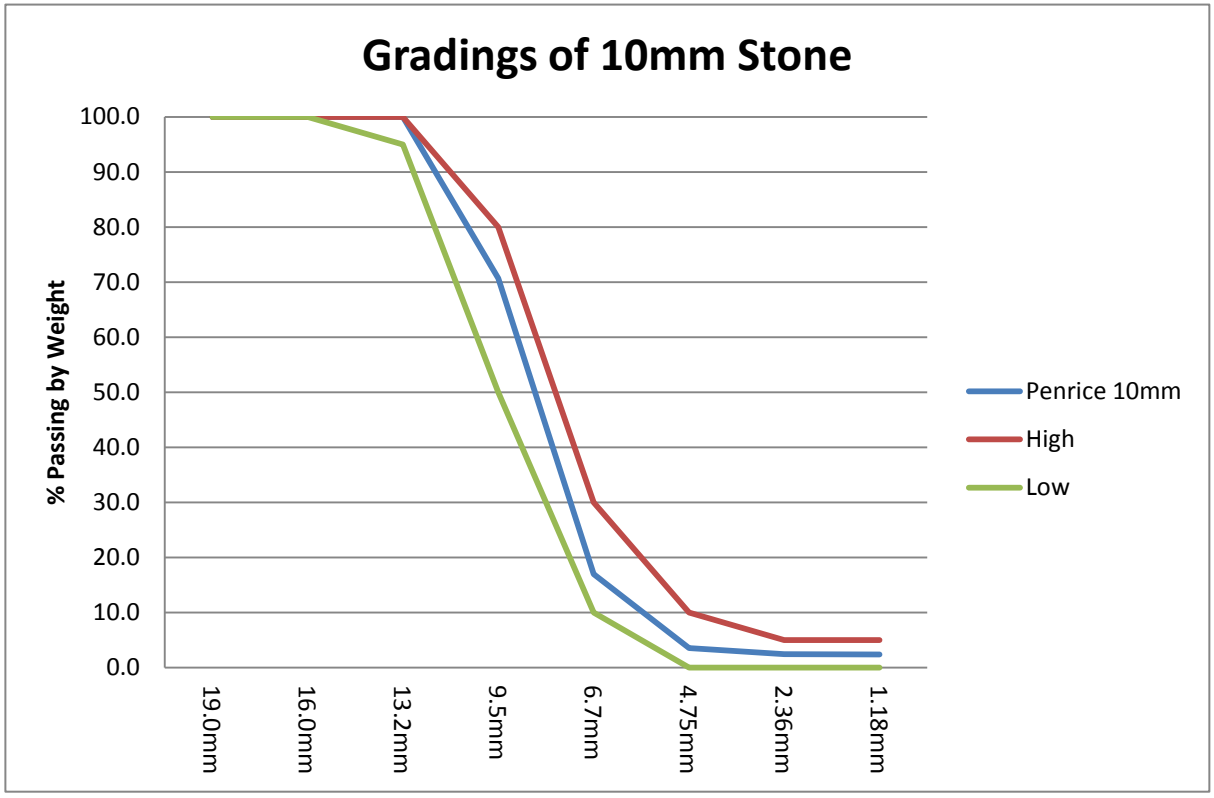

Figure 3.2 Grading of Penrice 10mm Stone Compared to Australian Standard

3.1.4 Titanium Dioxide

The Titanium Dioxide used for the laboratory trials was Degussa Evonik Aeroxide P-25. The product was supplied in 10Kg bags as shown in figure 3.3.
Aeroxide P-25 was selected as the titanium dioxide, as it is the industry standard for photocatalytic construction applications (Behnamann 2004; Chen & Poon 2009; Chen & Poon 2011; Chong *et al* 2010; Lackhoff *et al* 2002)

The characteristics of the Aeroxide are listed in the following table:

Table 3.6 Physical and Chemical Properties of the Titanium Dioxide (Source Degussa GmbH – Technical Data Sheet)

Properties	***Unit***	***Typical value***
Specific surface area (BET)	m^2/g	50 ± 15
Average primary particle size	nm	21
Moisture (2hrs at 105°C)	wt.%	≤ 1.5
Ignition loss (2hrs at 1000°C)	wt.%	≤2.0
pH (in 4% dispersion)		3.5 – 4.5
TiO_2	wt.%	≥99.50
Al_2O_3	wt.%	≤0.300
SiO_2	wt.%	≤0.200
Fe_2O_3	wt.%	≤0.010
HCl	wt.%	≤0.300
Sieve residue (45 µm)	wt.%	≤0.0500
Density	Kg/m^3	130

The Degussa Evonick Aeroxide P-25 has also been shown to be the most effective at the degredation of organic pollutants due to its crystal structure, 70% anatase, 30% rutile (Bahnemann 2004; Coleman *et al* 2007; Doll & Frimmel 2004; Lackhoff *et al* 2002).

Figure 3.3 TiO_2 P 25 (Guangzhou Huali Sen Trading Co., Ltd.)
Note: Guangzhau is a reseller of the Degussa P -25 TiO_2

3.1.5 Cost Analysis of Adding Titanium Dioxide to Concrete Mixes

The cost of TiO_2 can vary, depending on the crystal form, purity and photocatalytic reactivity. The average price for TiO_2 is $2.50 AUS/Kg - 2009. The standard price of Portland cement in Australia is $0.20 AUS/Kg - 2009. The addition of 10 percent TiO_2 to a 20MPa concrete, with a cementitious quantity of $260Kg/m^3$, will increase the cost by $65.00 AUS/$m^3$.
However, as TiO_2 has been traditionally used as a pigment in concrete, the construction industry is already paying the premium price for decorative and architectural concrete.

3.2 Epoxy Resin

The epoxy used for the image void determination was CONCRESIVE 2525, which was supplied by BASF Construction Chemicals. CONCRESIVE 2525 is a solvent free, high performance, low viscosity, two part epoxy. The characteristics are listed in the table below.

Table 3.7 Concresive 2525 Epoxy Resin Characteristics (Source BASF CC Australia – Technical Data Sheet)

Property	***value***
Colour	Clear/amber
Mix Ration (A:B)	3:1
Density	1.1Kg/L
Compressive Strength (7 days)	95 MPa
Viscosity	Unknown

3.3 Fluid Load

The deionised water used for cleaning and sample preparation for the fluid load was Diggers deionised water. The naphthalene used for sample preparation was Merck Schuchardt OHG > 99% pure.

3.4 Material Overview

In summary the materials in this research have been generally sourced from local suppliers and chosen because of previous research covered in the literature review. Although these materials are locally resourced, similar materials are widely available and can be sourced for photocatalytic permeable concrete applications.

4.0 Experimentation

4.1 Trial Mixes

The main objective of the research is to determine whether the addition of TiO_2 to permeable concrete would aid in the photocatalytic degradation of organic pollutants in water. To examine this, the mixes were designed in two parts. Firstly, the control mixes, which did not contain any TiO_2, with design void ratios of 30%, 25% and 20% were tested. Secondly, replication of the control mixes with varying additions of TiO_2 5%, 10% and 15% were tested. The control mixes were trials 1, 2, 3 and 13 in Table 4.1. All other mixes contained various amount of TiO_2 additions as shown in Table 4.1. Trial mix batch sizes were 60L. The mix designs are shown in Table 4.1.

Table 4.1 Mix Designs for all Trial Mixes

Trial	*Void Ratio Design*	*Cement*	*Aggregate*	*Water*	*W/C*	*TiO_2*	*TiO_2*	*Sand*	*Sand*
#	%	Kg	Kg	L		%	Kg	%	Kg
1	30	19.5	83.58	6.38	0.32	0	0	6.9	8.16
2	25	19.5	83.58	6.39	0.32	0	0	7.8	10.59
3	20	19.5	79.20	6.39	0.32	0	0	12	14.4
13	0	19.5	76.25	8.05	0.41	0	0	32.9	51.00
4	30	19.5	83.58	6.385	0.33	5	0.975	6.9	8.16
7	25	19.5	83.58	6.4	0.33	5	0.975	7.8	10.59
10	20	19.5	79.20	6.82	0.35	5	0.975	12	14.4
14	0	19.5	76.25	8.27	0.42	5	0.975	32.9	51.00
5	30	19.5	83.58	6.45	0.33	10	1.95	6.9	8.16
8	25	19.5	83.58	6.69	0.34	10	1.95	7.8	10.59
11	20	19.5	79.20	7.58	0.39	10	1.95	12	14.4
15	0	19.5	76.25	8.41	0.43	10	1.95	32.9	51.00
6	30	19.5	83.58	6.538	0.34	15	2.92	6.9	8.16
9	25	19.5	83.58	7.39	0.38	15	2.92	7.8	10.59
12	20	19.5	79.20	8.02	0.41	15	2.92	12	14.4
16	0	19.5	76.25	9.35	0.48	15	2.92	32.9	51.00

4.1.1 Mix Designs Combined Grading

The combined grading was calculated for all mix designs. The mix designs and grading were calculated using Microsoft Excel and were based on previous works (Kevern *et al* 2005; Lian , Zhuge & Beecham 2011; Zhuge 2007).

The combined grading analysis has been calculated for Trial 1, Trail 3 and Trail 13 and is shown in Figure 4.1. It is clear from the combined grading analysis that in Trail 1 there is only a small quantity of fine material in the mix.
The graph flattens out from 300um and less than 15% total passing at the 4.75mm sieve. The combined grading for all mix designs can be found in Appendix B.

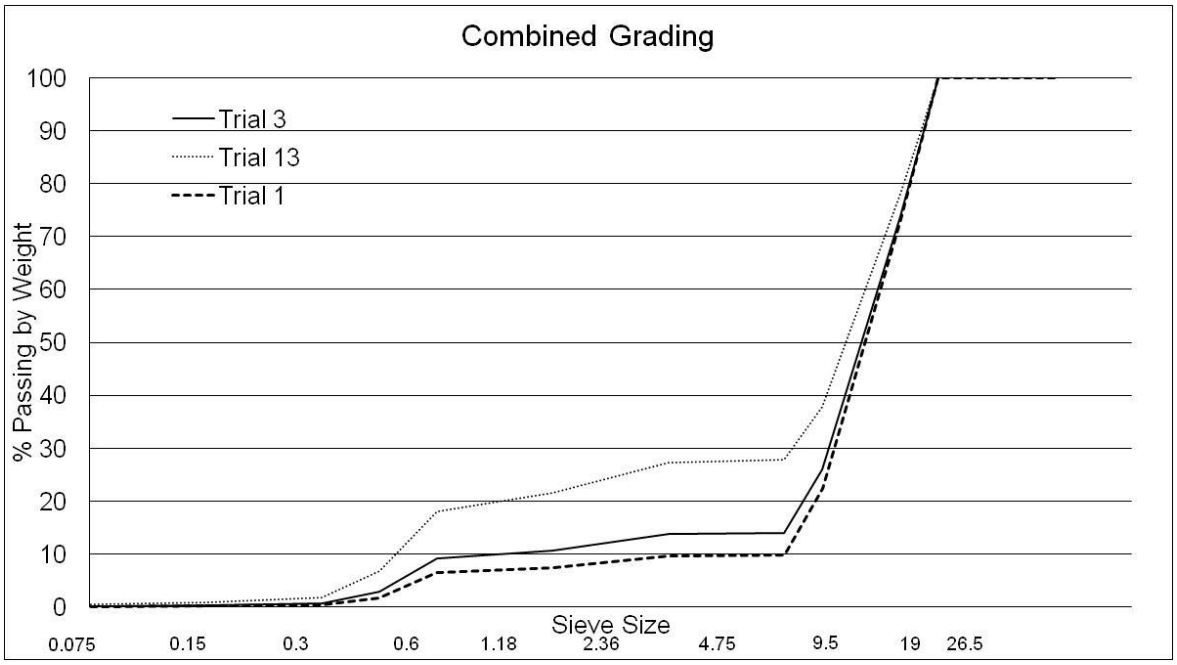

Figure 4.1 Combined grading Trials 1, 3 and 13

By comparing the combined gradings in Figure 4.1, it is very clear that Trial 13, which has a 0% void ratio, has significantly more total fine material than the others. It has approximately 45% passing at the 4.75mm sieve, compared to less than 20% and 15% for Trials 1 and 3 respectively. This is what differentiates a permeable concrete mix design to standard concrete mix design.

4.2 Batching Materials

A 120L Bennett pan mixer was used to batch the materials, as seen in Figure 4.2. All trial batches used the same sequence for mixing. Table 4.2 outlines that the trials were batched in accordance with AS 1012.2 -1994.

Table 4.2 Batching Sequence of Trial Mixes.

Time (Minutes)	***Procedure***
0	Course aggregate was placed in the static mixing bowl with fine aggregate on top.
0.5	Aggregates were mixed and 1/3 of the trial water was added to materials
1	Bowl is stopped. Cement and TiO_2 is added and aggregates are heaped over cement. Mixer is started and mixed for two minutes, whilst adding another 1/3 of batching water
3	Rest for two minutes
5	Mix for two minutes. Adjust remaining water to slump (if required).
7	Slump concrete

Figure 4.2 Bennett Mixer, Mixing Trial 1.

4.2.1 Admixtures in the Concrete

It was decided that chemical admixtures, such as platicisers and viscosity modifiers, would not be used in these trial mixes, as it was not known what effect their chemistry could have on the Photocatalyts. Even though the use of super plasticisers and viscosity modifiers has become common practice in enhancing the mechanical properties and workability of permeable concrete (AaMer *et al*, 2011), they have not been used in this research.

4.3 Sample Preparation and Testing Methods

4.3.1 Slump Test

Once the concrete had completed mixing a slump test was performed on the trial mixes. All slump tests were performed in accordance with AS 1012.3.1 -1998. An image of the slump test being performed on a trial can be seen in Figure 4.3.

The slump range achieved for desired workability was 0mm – 10mm. This is quite different to a standard structural concrete mix, which generally has a slump between 80mm -100mm. It is the low slump that aids in the formation of the voids.

Figure 4.3 Slump Testing on a Trial Mix

4.3.2 Casting of Concrete Mould

Traditionally concrete is cast into 100mm diameter by 200mm high moulds for concrete testing. However, it was decided that for repeatability and accuracy, the concrete would be cast into 1000mm X 600mm X 100mm moulds. The moulds were constructed with overlay plywood form ply which complied with AS/NZS2269 - 2004 and AS/6669 - 2007.

Before each mix the moulds were coated with a petroleum based concrete mould release agent, Rheofinish FR222, as per the manufacturer's instructions. The technical data sheet (TDS) can be found in Appendix A. The concrete was poured in two equal layers, with each layer being compacted lightly with a hand trowel, as seen in Figure 4.4 below.

Figure 4.4 First layer of concrete being cast into 1000mm X 600mm X 100mm mould

4.3.3 Curing

Samples were cured under laboratory conditions for a minimum of 28 days at 23°C ± 2°C and 50% ± 5% humidity.

4.3.4 Cutting Cores and Samples

After the samples had been cured for 28 days they were removed from their plywood moulds. 10 concrete cores were cut from the cast concrete samples with a Diteq Blu TS-162 core drill. A wet cut method was preferred, as shown in Figure 4.5. The samples then had approximately 15mm cut from either end of the core specimen to reduce edge effect. Rough 300mm X 300mm samples were cut from the cast concrete sample for the degradation analysis. These samples were later cut down to 200mm X 200mm samples with a Dewalt wet diamond blade saw at the Boral Construction Materials Laboratory in Stonyfell, South Australia.

Figure 4.5 75mm Cores Being Cut From Cast Concrete Sample.

Figure 4.6 75mm Concrete Cores

4.4 Mechanical Analysis

4.4.1 Compressive Strength

The compressive strength testing was performed on three 75mm cores per mix, (Figure 4.6). The core samples had dried out and required to be dampened with a wet cloth.
This was to bring the surface back to saturated dry before being weighed with an A&D Mercury balance and measured with an Intech digital vernier caliper to calculate the density.

The compressive strength testing of the cores was done in accordance with the following Australian Standards; Australian Standard 1012.12.1 – 1998- Method for Testing Concrete - Determination of Mass Per Unit Volume of Hardened Concrete – Rapid Measuring Method, Australian Standard 1012.9 – 1999- Method of Testing Concrete – Determination of Compressive Strength of Concrete Specimens, Australian Standard AS 1012.14-1991- Method for Testing Concrete – Method for Securing and Testing Cores from Hardened Concrete for Compressive Strength. The samples were immersed in a 23°C water curing tank for 3 days. The samples were then removed and sulfur capped at both ends. A compressive strength testing machine was used to determine the compressive strength of the cores. A factor was applied for the core dimensions

4.5 Hydraulic Property Testing – Permeability

As highlighted in the literature review, permeability is a key factor in permeable concrete breaking down inorganic pollutants and in consequently replenishing the underground water supplies.

Recently, Lian, Zhuge & Beecham (2011) compared the falling head method and constant head method for determining the permeability of permeable concrete. Their findings showed that the constant head method was more suitable for permeable concrete and that the constant head level appeared to have less effect on variation of the results. The two methods have been used to determine the permeability (k) of the concrete mixes.

4.5.1 Falling Head Method

The samples were sealed inside a flexible pipe as shown in Figure 4.7. Four litres of water were poured into the cylinder just above h_1. When the meniscus dropped to h_1 the time was recorded that it took to reach h_2. This process was repeated 3 times per concrete core to establish the permeability.

The coefficient of permeability (k) was determined by the following equation:

$$k = \frac{aL}{At} \ln\left(\frac{h_1}{h_2}\right) \tag{4.1}$$

k = coefficient of permeability, cm/s
a = cross sectional area of stand pipe
A = Cross sectional area of specimen
L = length of sample
T = time in seconds from H1 to H2
h_1 = initial water level
h_2 = final water level

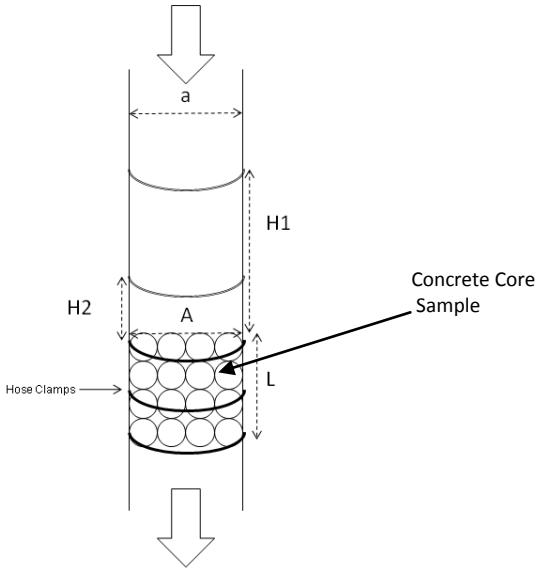

Figure 4.7 Falling Head Apparatus

4.5.2 Constant Head Method

The constant head test was performed with the testing device as shown in Figure 4.8. This device was adopted from a similar design recommended by the Japanese Concrete Institute (Park *et al* 2009).

Water was continuously pumped into the sample chamber until a continuous flow was achieved from the overflow outlet and collection outlet. Once no air bubbles were present in the collection outlet, the water was collected for 60 seconds. The permeability coefficient was calculated using equation 4.2.

$$k = \frac{L \times Q}{H \times A(T_2 - T_1)} \quad (4.2)$$

k = permeability coefficient, cm/s
L = length of sample, cm
Q = flow quantity during period time T_1 to T_2, cm^3
H = drop height, cm
A = cross section area of test sample, cm^2
T_1 = measurement starting time, s
T_2 = measurement completed time, s

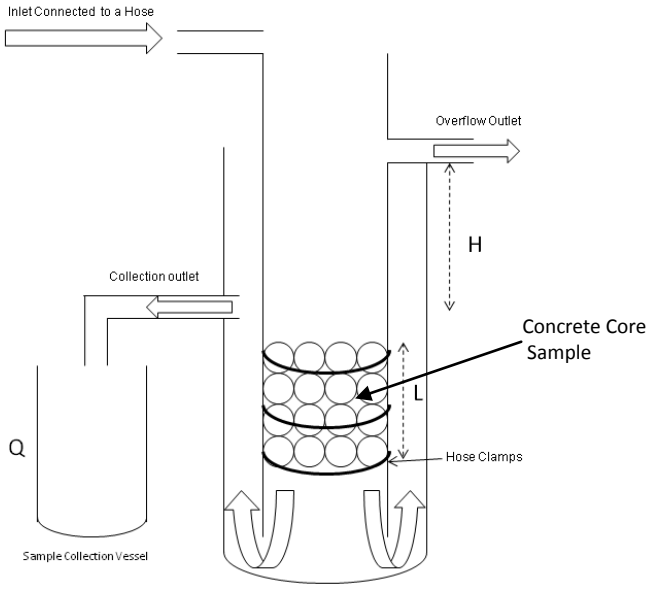

Figure 4.8 Constant Head Set Up

4.6 Void Determination

Research by Marlof *et al* (2004), suggests that image void analysis is more accurate to determine void ratio than the standard displacement test. Therefore, both test methods have been trialed to determine which method is the most effective and practical for photocatalytic permeable concrete void ratio analysis.

4.6.1 Void Ratio - Image Analysis Method

4.6.1.1 Equipment

- 75mm poly pipe
- duct tape
- 5L mixing jug
- Epoxy resin part A and B
- Bosch electric drill
- Mixing paddle
- Rubber mallet
- Diamond Wet cut saw
- Canon MP490 flat bed scanner
- Adobe Photoshop Extended
- Computer

4.6.1.2 Casting with Epoxy Resin

75mm diameter poly pipes were cut into 150mm lengths and taped to seal the bottom of the pipes. A single core sample was placed inside the pipes and placed vertically on a flat bench-top. The low viscosity epoxy CONCRESIVE 2525 part A was poured into a 5L jug then followed by CONCRESIVE 2525 part B, which was mixed in and stirred for two minutes with an electric drill and paddle. The epoxy was then poured into the pipes slowly, whilst being tapped with a rubber mallet to remove any air bubbles. The specimens were left undisturbed for 24 hours, allowing the epoxy to harden. After the epoxy had hardened, the moulds were cut on a Dewalt wet diamond saw into 20mm lengths as shown in Figure 4.9.

Figure 4.9 Cut Segment of Trail Core 3

4.6.1.3 Image Analysis

The slices were then placed on a Canon MP490 flat bed scanner, scanned at 600 dpi in black and white mode. The image was saved as a *.BMP file. The file was then opened with Abode Photoshop CCS Extended. All images were cropped using a-elliptical marquee tool as seen in Figure 4.10. All cropped images can be viewed in Appendix C.

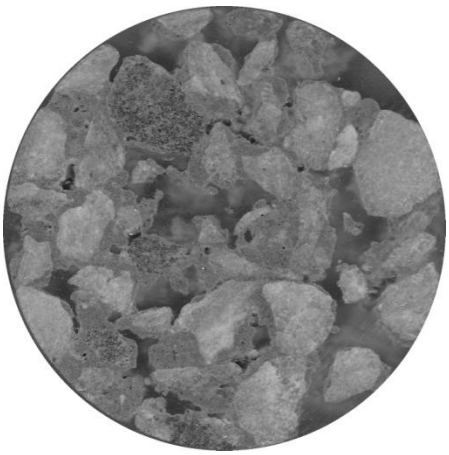

Figure 4.10 Cropped Image of Trial Core 3, Segment 3

To distinguish between the epoxy filled voids and the aggregate and paste, the image levels were manipulated as seen in Figure 4.11. The image was then converted from RGB to Greyscale. To remove any undefined areas such as paste, which appear as grey pixels, the image level was adjusted once more.

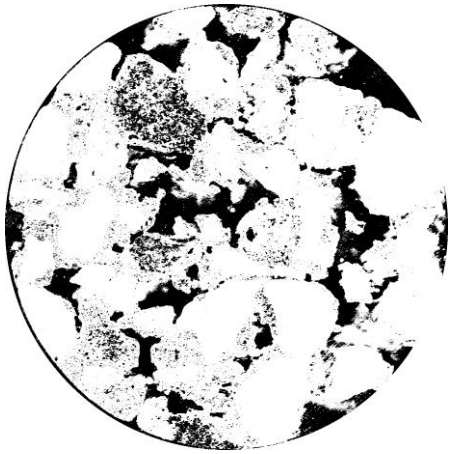

Figure 4.11 Image analysis of Trail Core 3, segment 3

Finally, the elliptical marquee tool was reapplied over the image to determine the total number of pixels in the core. The pixel count and the manipulated images for all cores can be found in Appendix (C). The total amount of black pixels, which represents the epoxy filled voids, was calculated from the histogram.

The void ratio was calculated using the following formula;

$$Void\ Ratio\ (V_r)\ = \frac{Black\ Pixels}{Total\ pixels} \times 100\% \qquad (4.3)$$

4.6.2 Void Ratio - Standard Void Method

The standard void ratio was tested by first drying the cores in a 105°C oven for 24 hours. The samples were then allowed to cool back to room temperature in a dessicator, then weighed to determine their dry weight (W_2). The samples were then submerged into a 23°C water-bath for 5 minutes and turned several times to allow all air bubbles to escape. Then the weight was determined by using a specific gravity balance set up (Figure 4.12). The samples were placed into the cradle whilst under water. The mass of the sample was then taken whilst submerged (W_1).

Equation 6 determines of the standard void ratio:

$$V_r = [1 - \left(\frac{W_2 - W_1}{P_w\ Vol}\right)] X\ 100(\%) \qquad (4.4)$$

Where:
W_1 = dry weight Kg
W_2 = wet weight Kg
Vol = Volume of sample Kg/m^3
P_w = density of water Kg/m^3

Figure 4.12 Specific Gravity (http://www.testinginstrumentsindia.com/equipment-instruments.html 8/2/2012 - Associated Scientific and Engineering works)

4.6.2.1 Equipment for Standard Void Method

The following equipment was used for the standard void analysis.

- 105°C Oven
- Analytical Balance 0.01g
- Specific Gravity Balance
- Temperature probe
- Dessicator with silica gel

4.7 Degradation Analysis

4.7.1 PAH Degradation Testing Apparatus

As stated in the Literature Review, there has been very little research conducted on photocatalytic construction materials degrading organic pollutants in water and even less on using photocatalytic permeable concrete.
Therefore no testing apparatus have previously been used for simulating this test. The following design, Figure 4.13 and Figure 4.14, was used for the degradation analysis.
This was based on research presented by Bahnemann (2004), applying a photocatalytic reticulation system testing apparatus for water treatment testing.

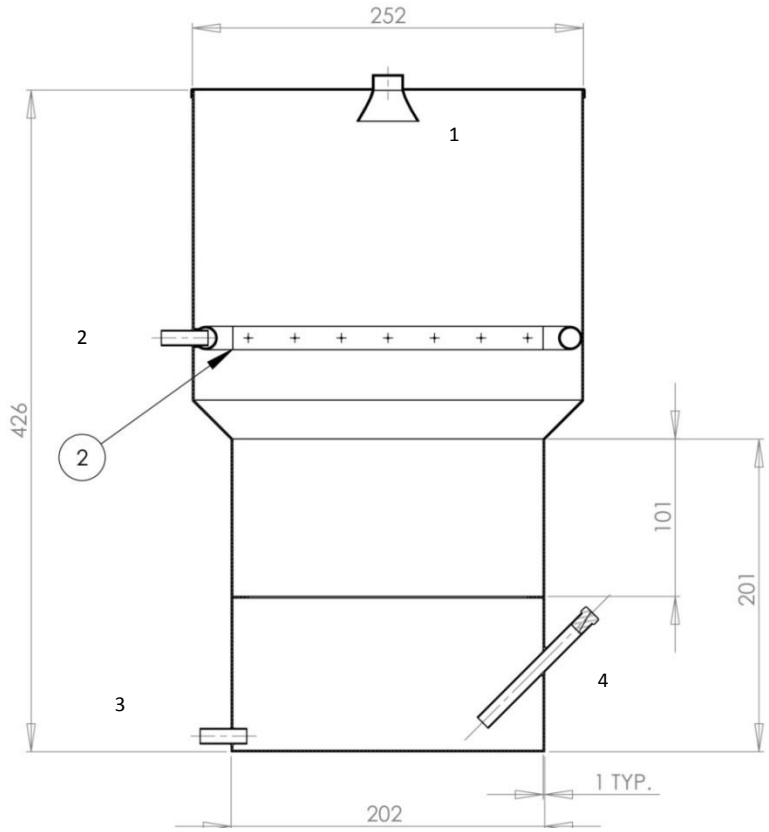

Figure 4.13 TiO_2 Testing Apparatus

Key components:
1.) UV Lamp
2.) Sample Inlet and sprayer
3.) Sample outlet
4.) Sampling point

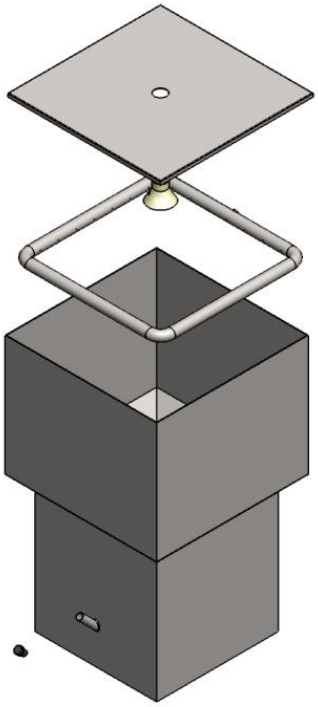

Figure 4.14 Housing and Assembly of TiO_2 Testing Apparatus

The testing apparatus was made of M16 stainless steel and constructed by Adam's Fabrication in Adelaide, South Australia. The water inlet pipe connected to the 15mm Φ injector tube, which sat 140mm above the concrete sample. The injector tube had 2mm Φ holes every 30mm to allow the pumped solution to flow onto the concrete mould. Above the injector pipe was the lid, which was sealed with a rubber gasket and duct tape. In the lid was a Phillips Actinic BL TL 8 Watt UV with a UV – A radiation in the 350 – 400nm range (Figure 4.15). The concrete test specimens sat on 4 stainless steel 10mm lugs which stopped it going in the reservoir at the bottom of the apparatus. On the side of the apparatus there was a 10mmΦ x 100mm long sampling point, which allowed samples to be taken from the reservoir with a pipette. When not in use the sampling point was sealed with a rubber bung.

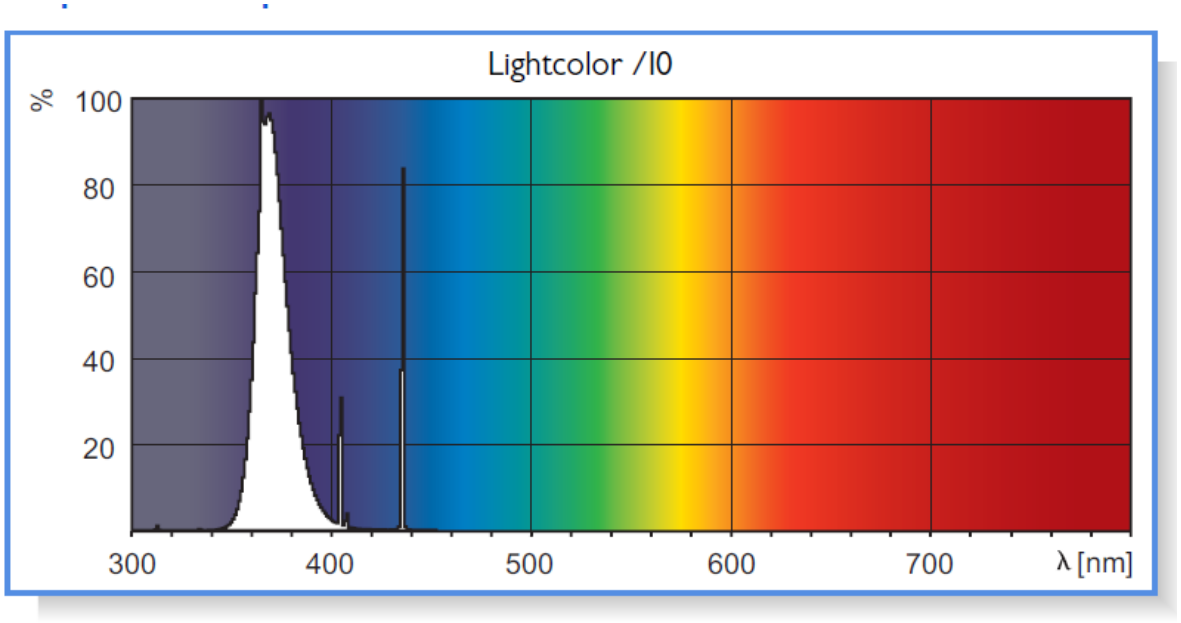

Figure 4.15 Spectrum of Light Globe Used

4.7.2 Fluid Load, Naphthalene Sample Preparation

A 50µg/L concentration of naphthalene was used, as studies by Eriksson *et al* 2007, Gobel, Dierkes & Coldeway 2006 and Schipper *et al* 2007, have shown that storm water samples taken from the side of roads had PAH present in concentrations between 50µg/L and 20µg/L. Naphthalene was the PAH chosen, as it is the simplest and most soluble in water. It also has relatively low toxicity compared to other PAHs which are generally classed as known carcinogenic and mutagenic compounds.

The sample was prepared using the following method:

1) Approximately 0.00010 grams of Naphthalene was weighed on a Mettler AE 160 analytical balance.
2) 500ml of 4L deionised water was placed into a 2 L volumetric flask.
3) The sample of Naphthalene was then washed with 1 litre of deionised water into the volumetric flask.
4) The volumetric flask was then filled to 90 percent with deionised water, sealed and allowed to stand.
5) After 1 hour the sample was topped up and used immediately.

4.7.3 Testing Degradation of Naphthalene in the Apparatus

The testing apparatus was set up in a 23°C ± 2°C, 50% ± 5% humidity temperature controlled analytical laboratory as shown in Figure 4.16.

Figure 4.16 Photocatalytic Testing Apparatus

The testing apparatus was connected to an Onga –Riva Flow, 0.33HP pump through clear chemical resistant hosing. The pump was set to a flow rate of 3L/min and was checked before each trial. Before each test 1 litre of deionised water was reticulated through the system to clean it out and ensure everything was running correctly.

After the apparatus had been cleaned and set up, the Naphthalene sample was poured into the apparatus, sealed and allowed to run for 5 minutes. The initial sample was then taken and the pump was turned off.
A concrete sample was then placed inside the apparatus, the lid was closed and sealed with tape, the pump was turned back on and finally the UV light was turned on. The apparatus was not turned off during any of the testing runs.

4.7.4 Sampling of Fluid Load

At each hourly time interval the following method was used to sample the material and test the temperature and pH.

1) A 20ml syringe was cleaned 3 times with deionised water before removing a 20ml sample from the sampling point on the apparatus and placed in a glass beaker.
2) The sample was immediately tested for pH and temperature using a Eutech pH metre and temperature probe.
3) A 100ml syringe was cleaned 3 times with deionised water before removing a 100ml sample from the sample point on the apparatus.
4) The 100ml sample was placed into a 1 litre semi volatile organic bottle, then labelled and sealed.

4.7.5 Gas Chromatography Mass Spectrometer Analysis

The samples were sent to MGT Labmark Environmental Laboratories for quantitative analysis. The samples were tested using the USEPA 8270D "Semi Volatile Organic Compounds by Gas Chromatography / Mass Spectrometry (GC/MS)" method. This method is designed to extract samples of semi volatile organic compounds from various solid waste matrices, soils, air sampling media and water samples. The samples were able to be directly injected to the Gas Chromatograph, where they passed through a narrow-bore fused-silica capillary column, which was temperature-controlled and programmed to separate the analytes. The analytes then passed through the column at different rates into the Mass Spectrometer for quantitative and qualitative analysis. The following diagram, Figure 4.17, shows the equipment used.

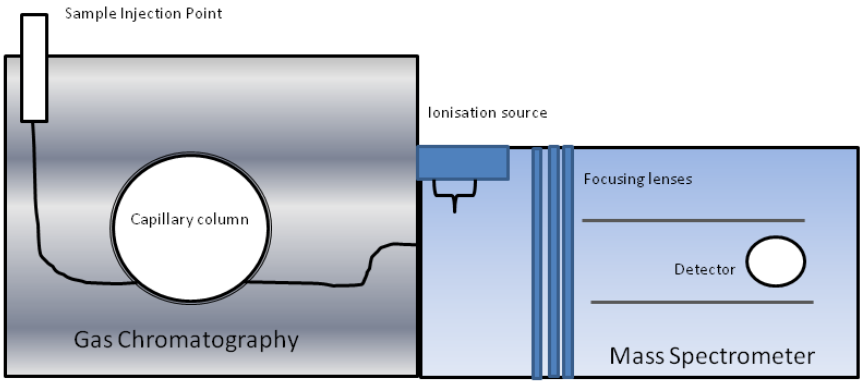

Figure 4.17 Gas Chromatography Mass Spectrometer

Determining the mechanical properties of photocatalytic permeable concrete are important for engineers to be able to specify this type of concrete in future projects. Some of the test methods used have been adapted from other industries, as certain tests methods do not exist for photocatalytic permeable concrete.

5.0 Results and Discussion

All hydraulic and mechanical testing results for this research are displayed in the following Table 5.1.

Table 5.1 Overview of Hydraulic and Mechanical Testing Results

Trial	*% TiO_2*	*W/C*	*Design Voids*	*Hydraulic Testing*				*Mechanical Testing*	
				Standard test	*Image analysis*	*Permeability Falling Head (k)*	*Permeability Constant Head (k)*	*Compressive Strength*	*Density*
			%	*% Void*	*% Void*	*mm/s*	*mm/s*	*MPa*	*Kg/m^3*
1	0	0.32	30	31	32	15.9	6.12	8.3	1757
2	0	0.32	25	26	28	12.4	5.0	10.0	1839
3	0	0.32	20	22	22	7.1	3.94	12.5	1944
13	0	0.41	0	0	0	0	0	15.8	2181
4	5	0.33	30	31	30	21.0	6.66	5.7	1713
7	5	0.33	25	29	30	11.8	6.50	6.5	1711
10	5	0.35	20	24	23	10.0	5.0	8.2	1754
14	5	0.42	0	0	0	0	0	11.0	2152
5	10	0.33	30	30	31	15.5	5.37	4.0	1687
8	10	0.34	25	33	30	13.8	5.59	5.6	1569
11	10	0.39	20	21	21	4.8	3.71	9.6	1924
15	10	0.43	0	0	0	0	0	13.0	2247
6	15	0.34	30	33	30	7.3	3.38	3.3	1603
9	15	0.38	25	26	24	3.4	3.55	7.7	1807
12	15	0.41	20	17	16	2.2	1.4	14.0	1979
16	15	0.48	0	0	0	0	0	12.3	2047

5.1 Casting

5.1.1 Mixing

During the trials it was observed that the addition of TiO_2 significantly reduced the workability of the concrete compared to the control mixes, which did not contain TiO_2. To try and maintain the same workability as the control mixes, more water was added to the concrete mixes, which increased the water cement ratio (Table 4.1 and Table 5.1). The slump test was used as a measure of concrete workability. There were no other changes to the mixes from the control trials it is assumed that the fineness and low density of the photocatalytic TiO_2 caused the loss in workability and poor rheology of the mix.

5.1.2 Casting

Due to the poor workability of the TiO_2 mixes, 4 - 12 and 14 – 16, the compaction when casting was not as efficient as the control mixes. This may highlight the need to add chemical admixtures to improve the concrete workability and paste rheology, when using fine material for improved compaction and mechanical properties.

5.2 Void Analysis

It is well documented that the porosity of permeable concrete is closely related to the void ratio and that to achieve a permeability coefficient greater than 0.01m/s, it is recommended that the void ratio be 20 to 29% (Neithalath, Weiss, Olek 2009).

The control mixes, Trials 1, 2 and 3 were designed to have a void ratio of 30%, 25% and 20%. The control mixes achieved very similar results for the standard void test and the image analysis test, (Figure 5.1), with the void ratio being almost the same as the theoretical design. As the results were similar to the design, this gave confidence in the compaction method used to cast the moulds as research by Chindaprasirt *et al* (2006), Putman & Neptune (2010) and Deo & Neithalath (2011), showed poor compaction resulted in undesirable void ratios and poor mechanical properties.

When comparing the standard void ratio analysis to the image analysis test for the control mixes, (Figure 5.1), there was only a slight increase, with the highest being 2% for trial 2. This slight variance could be because the image analysis is able to measure "dead end" pores. Similarly, Safiuddin & Hearn (2004) showed that water could not completely fill the voids, as small air pockets had been trapped in the voids under standard atmospheric conditions, as per Figure 5.2.

The results showed that for the control mixes, the image analysis test was slightly more accurate than the standard void test. However, the image analysis was a far more time consuming test compared to the standard void test. Therefore, for a relatively accurate analysis with quick results, the standard test has shown to be an effective test method for determining void ratio.

The image analysis and standard test method for measuring the porosity of permeable concrete have been found to have a reasonable correlation. Marlof *et al* (2004) have drawn similar conclusions from their research.

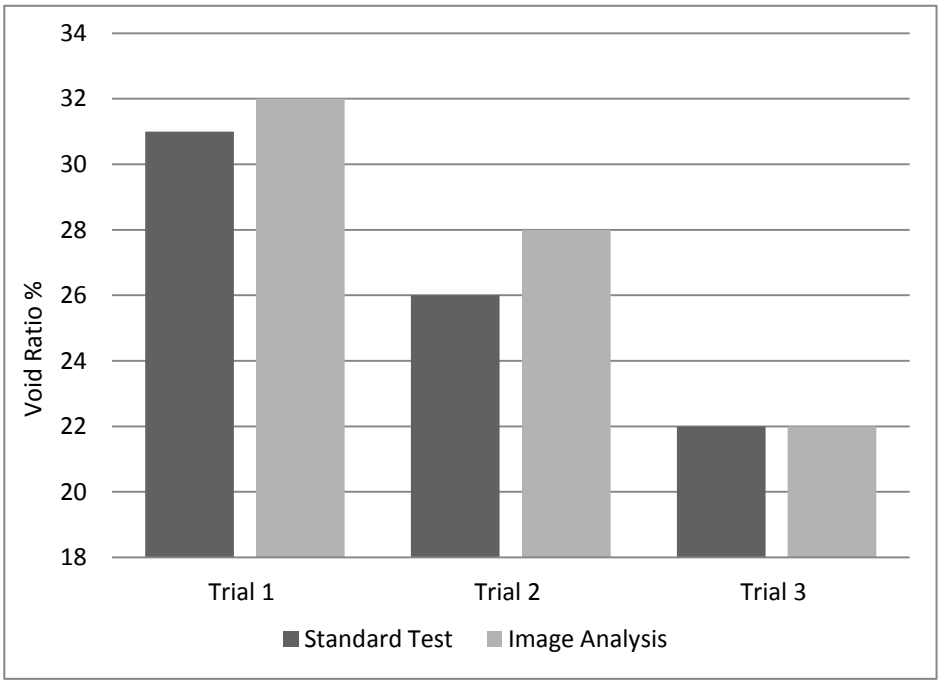

Figure 5.1 Void Ratio Control Mixes 1,2,3

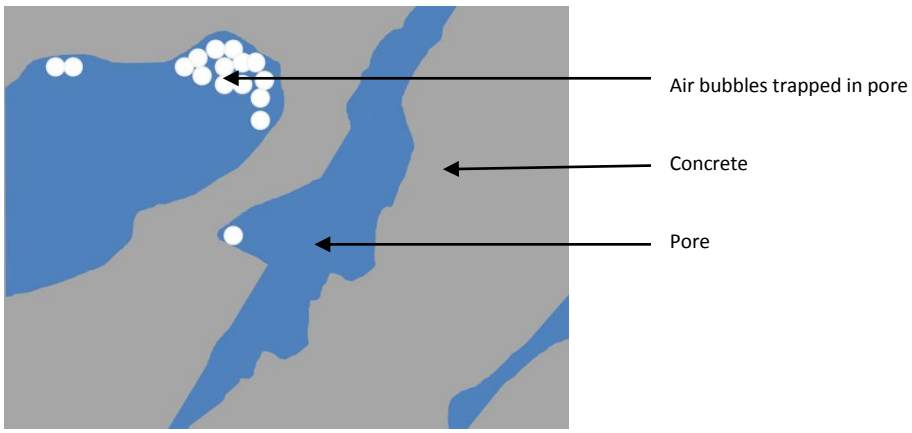

Figure 5.2 Air Bubbles Trapped in Dead End Pore

To adjust the void ratio, the control mixes had varying additions of fine aggregate (sand) added to the mix. Trial 1 had 6.9% sand addition by weight of total aggregates, Trial 2 had 7.8% sand and Trial 3 had 12% addition to the mix. Although, Trial 3 had 5.1% more fine material in the mix compared to Trial 1, the loss in void ratio was less than 10%.
Similarly, Kevern *et al* (2005) added 7% additions of sand to permeable concrete and only reduced the void ratio by less than 10%. The relationship between sand addition and void ratio produce a linear response, (Figure 5.3), the void ratio for Trail 13 was assumed to be 0 percent as the concrete specimen was a solid mass. Similarly Wang *et al* (2006) achieved an R^2 value of 0.92 for percentage voids versus percentage sand addition. These findings will hopefully aid engineers when designing permeable concrete to have desired void ratios.

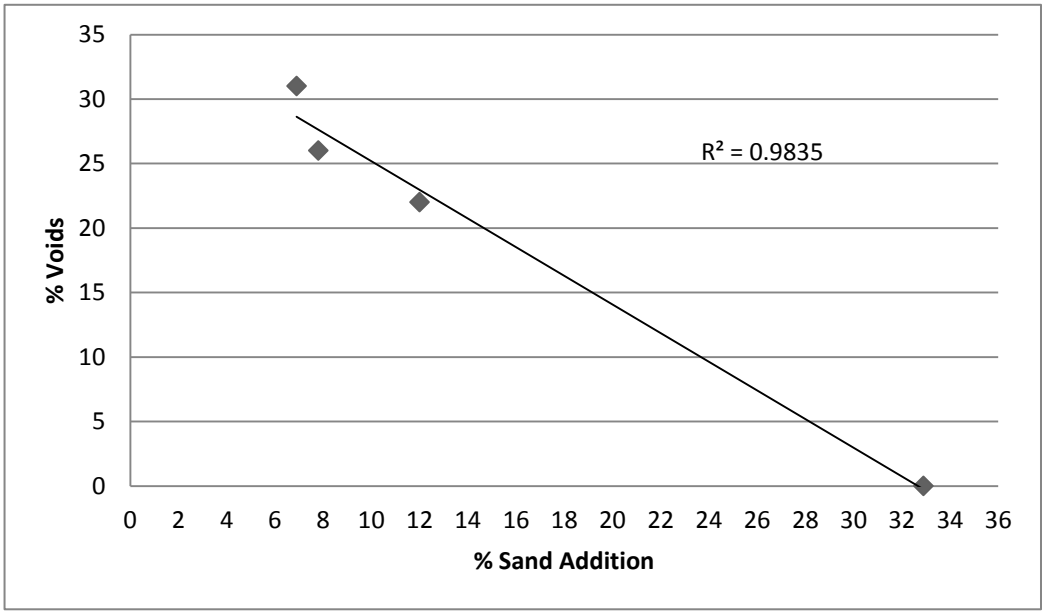

Figure 5.3 Sand Addition Affecting Void Ratio

Figures 5.4, 5.5 and 5.6 compare the control mixes to their TiO_2 addition mixes. The mix design of 30% void ratio shows that the addition of TiO_2 had very little effect on the void ratio. Both the image analysis and standard void ratio produces very similar results, especially for the 30% design void ratio.

When examining the 25% void ratio mixes in Figure 5.5, it appears that with both test methods, the 5% addition of TiO_2 slightly increased the void ratio by approximately 2%. This may be explained due to the reduction in compaction, caused by the poor workability that the TiO_2 caused, as previously discussed. The standard void test for Trial 8 produced a void ratio of 33% compared to the control mix of 26%. However, the image analysis only showed that there was a 2% difference between the Trial 8 and the control.

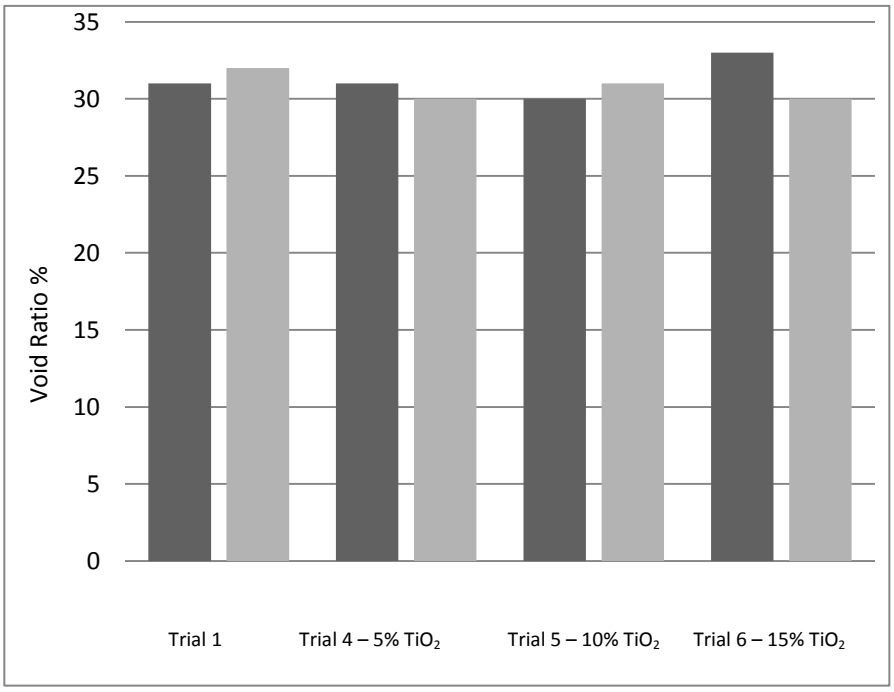

Figure 5.4 Void Ratio Trials 1, 4, 5 and 6 – Design Void Ratio 30%

After examining the core samples of Trial 8 they appeared to be very poorly compacted, creating large dead end voids. Overall, it appeared that the addition of TiO_2 did not significantly reduce the void ratio. In fact, it may have increased the void ratio initially, due to the poor workability of the mix, which was created by the TiO_2.

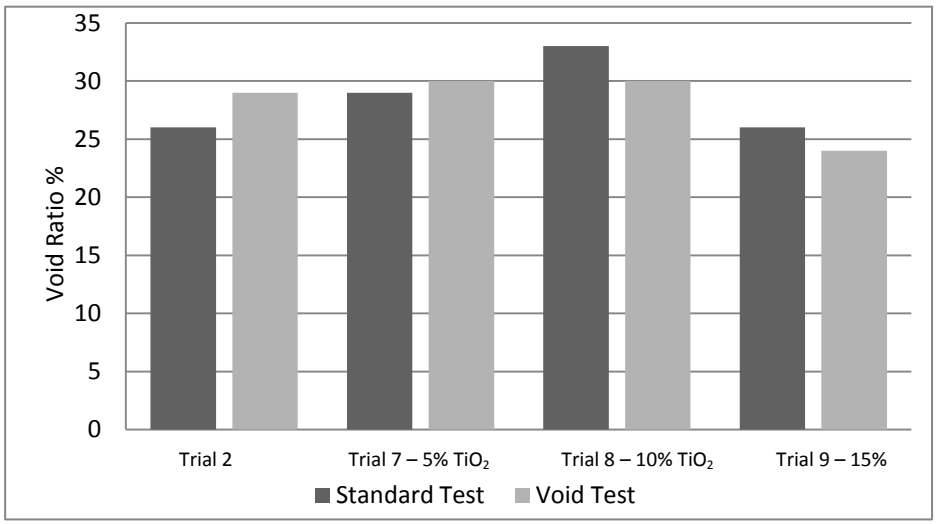

Figure 5.5 Void Ratio Trials 2, 7,8 ,9 – Design Void Ratio 25%

Another interesting trend was noticed when examining the epoxy filled segments from the image analysis method. The network of voids that made up the permeable concrete did not appear to be uniform throughout the concrete, (Table 5.2). A trend was noted, that the middle of the core appeared to have a higher void ratio than the top and bottom.

Table 5.2 Segment Analysis for Epoxy Void Ratio Test

Segment	***Trial 1 Core 1***	***Trial 7 , Core 3***	***Trial 11, Core 3***
	% Void Ratio	***% Void Ratio***	***% Void Ratio***
Top -1	22	21	19
Middle -2	32	50	33
Bottom -3	27	38	19

The void ratios presented in Figure 5.6 exhibited a similarity to Trials 4, 5 and 6, as the addition of TiO_2 initially appeared to increase the void ratio by 2%. The relationship between the 5%, 10% and 15% addition of TiO_2 to the void ratio was shown to be linear for Trials 10, 11 and 12, (Figure 5.7).

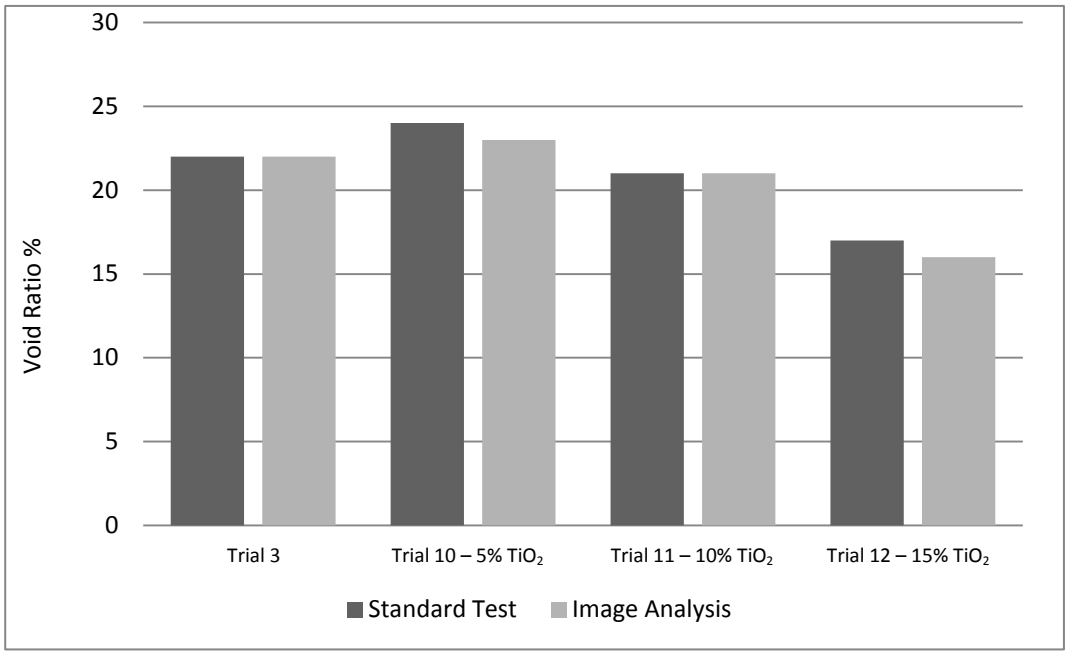

Figure 5.6 Void Ratio Trial 3, 10, 11, 12 – Design Void Ratio 20%

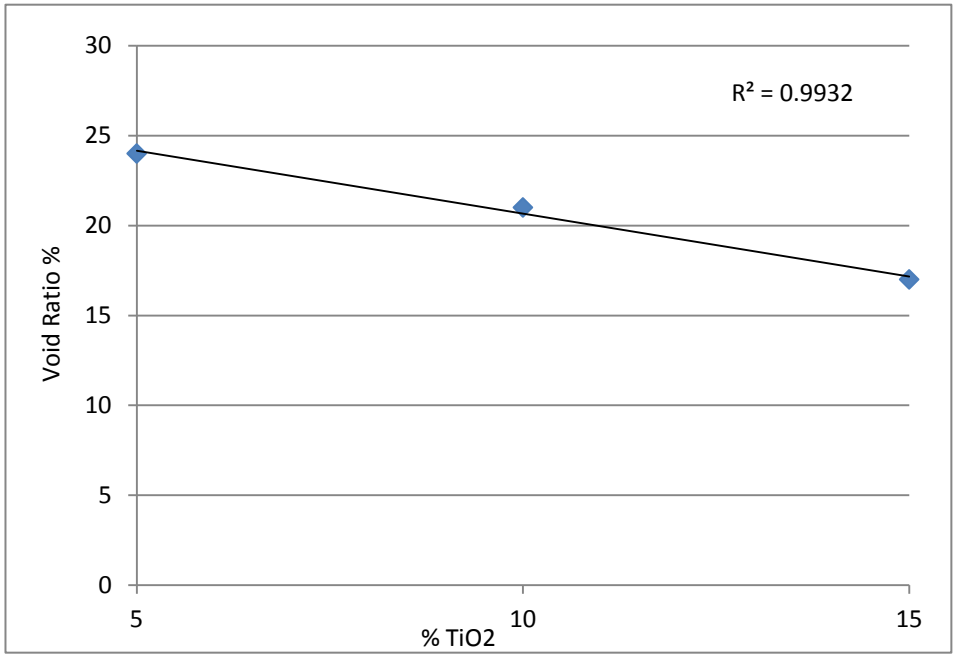

Figure 5.7 Trials 10, 11 and 12 Standard Void Ratio Test

5.3 Permeability

5.3.1 Falling Head

Fundamentally, permeability rate (k) is what makes permeable concrete pavement unique when comparing it to standard concrete pavement. There is little or no research available on what effect the addition of TiO_2 would have on permeability, for either test method. The Falling Head results in Figure 5.8 and Table 5.3, showed a trend whereby increasing the amount of TiO_2 reduced the permeability. This result was expected, as research by Kevern *et al* (2005) had shown that increasing the addition of fine materials reduced the permeability. The table below shows the percentage reduction of permeability caused by the addition of TiO_2.

Table 5.3 Permeability Reduction by TiO_2 Addition Compared to the Control Mixes –Grouped in Original Mix Designs

Design Void Ratio	***0% TiO_2***	***5 % TiO_2***	***10% TiO_2***	***15% TiO_2***
%		***% K value of Control***	***% K value of Control***	***% K value of Control***
30	100%	+32	-3	-46
25	100%	+5	+11	-27
20	100%	+41	-22	-31

Note: (+) indicates that there has been an increase in permeability compared to the 0% TiO_2

(-) Indicates there has been a decrease in permeability compared to the 0% TiO_2

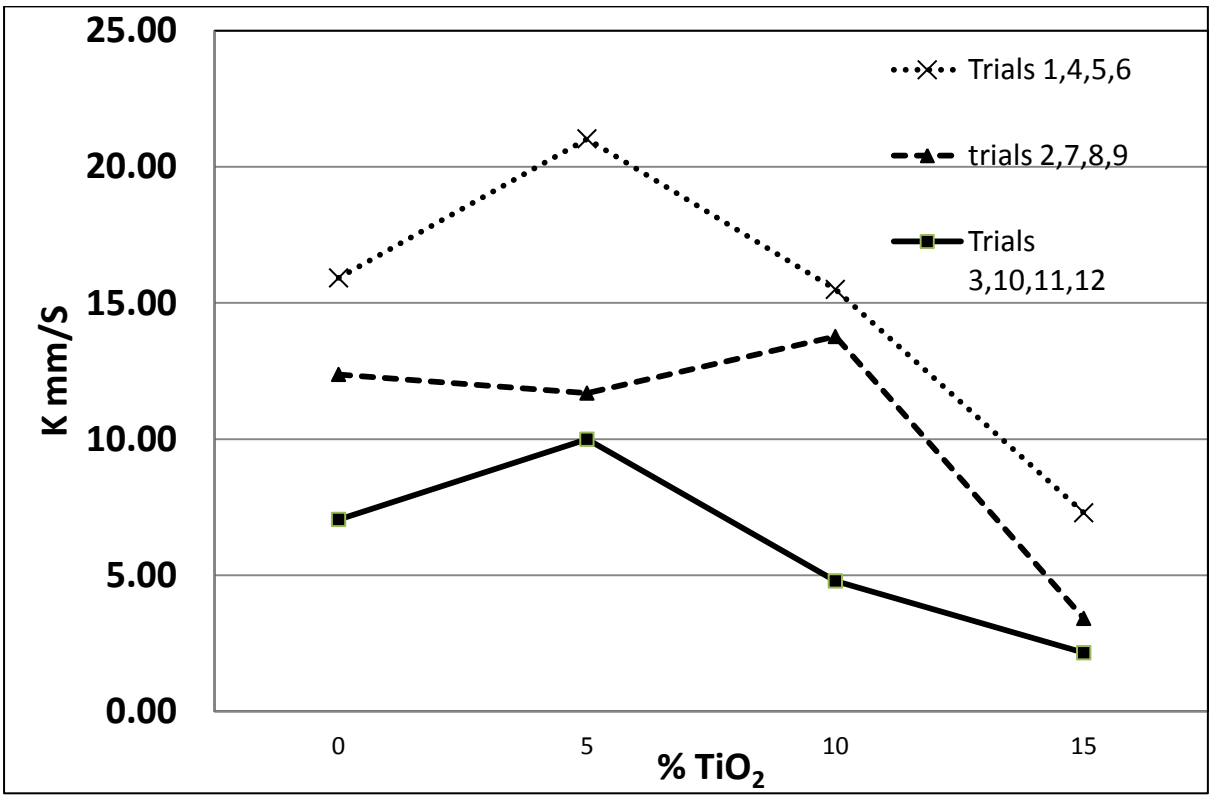

Note: Trials 1,4,5,6 orinigal mix design was 30% Void Ratio
Trials 2,7,8,9 original mix design was 25% Void Ratio
Trials 3,10,11,12 original mix design was 20% Void Ratio

Figure 5.8 Falling Head Results Grouped in Original Mix Designs

There is a relationship between void ratio and permeability, which is that higher void ratios have higher permeability (Kevern *et al* 2005; Wang *et al* 2006). As discussed previously, the void ratio of the photocatalytic concrete was significantly changed when compared to the control mixes this was due to the poor compaction caused by the reduced rheology in the wet mix. Therefore, as permeability is a function of void ratio, the photocatalytic concrete needed to be grouped together as per their actual void ratio, not their theoretical mix designs (table 5.4).

Table 5.4 Normalized Permeability Results for Falling Head Method

Trial Number Grouped	*Void Ratio %*	*0% TiO_2 (K) Falling head*	*5% TiO_2 (K) Falling head*	*10% TiO_2 (K) Falling head*	*15% TiO_2 (K) Falling head*
1,4,5,6,7,8	30	15.92	16.36	14.635	7.29
2,9,10	25	12.38	9.99	-	3.4
3,11,12	20	7.05	-	4.79	2.15

It is obvious in Figure 5.9 that the addition of TiO_2 reduces the permeability, especially with the 15% TiO_2 addition. It is accepted that the permeability of permeable concrete ranges from 0.2cm/s to >1.0cm/s for the Falling Head Method (Haselbach, Valavala & Montes 2006). Therefore, even though the addition of TiO_2 had reduced the permeability of the photocatalytic permeable concrete, it is still applicable, as the permeability was greater than 0.2cm/s for the Falling Head method. It can be concluded from Figure 5.9, that the 20% and 25% void ratio appear to have a linear relationship between TiO_2 addition and permeability; however this is not the case for the 30% voids.

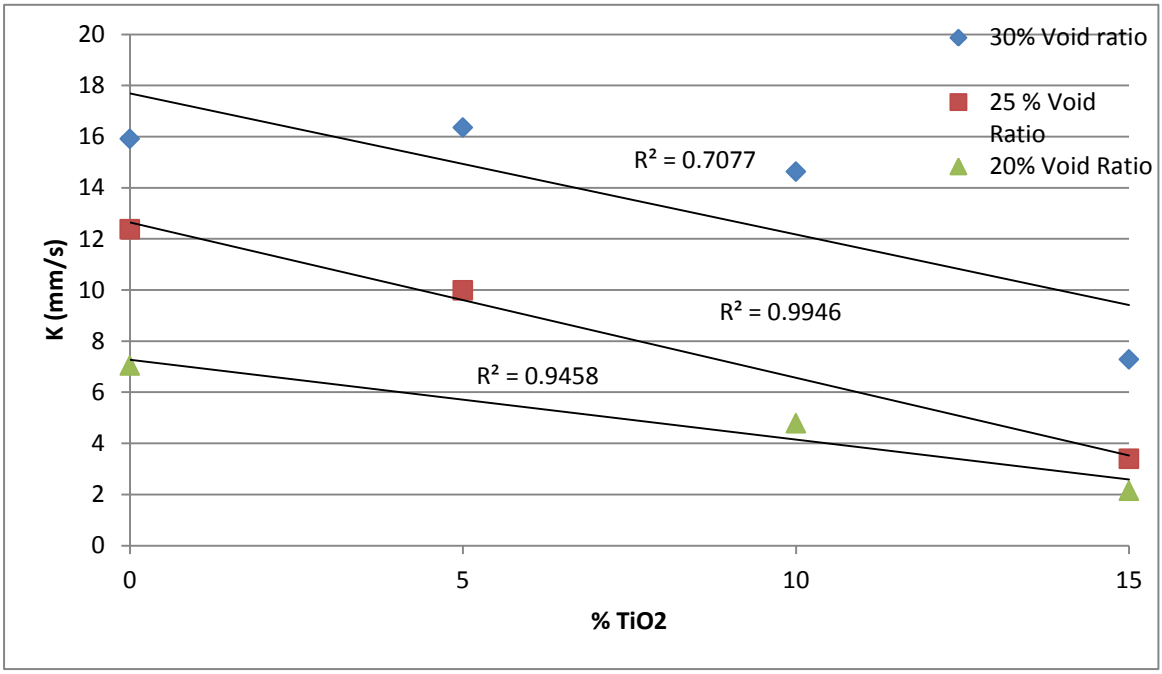

Figure 5.9 Normalised Permeability Falling Head Method

5.3.2 Constant Head

The Constant Head Method produced a similar trend to the Falling Head method as shown in Figure 5.10. It demonstrated, that compared to the design control mixes, there was an initial increase in permeability for the 5% addition for all three design void ratios. The increase in permeability was a result of the increase in void ratio, caused by the poor compaction, as a result of the TiO_2 addition.

It is well known that permeability is a function of void ratio, this is evident in the results displayed in Figure 5.10. However, when the TiO_2 was introduced into the permeable concrete this changed the void ratio and hence the permeability, Figure 5.11.

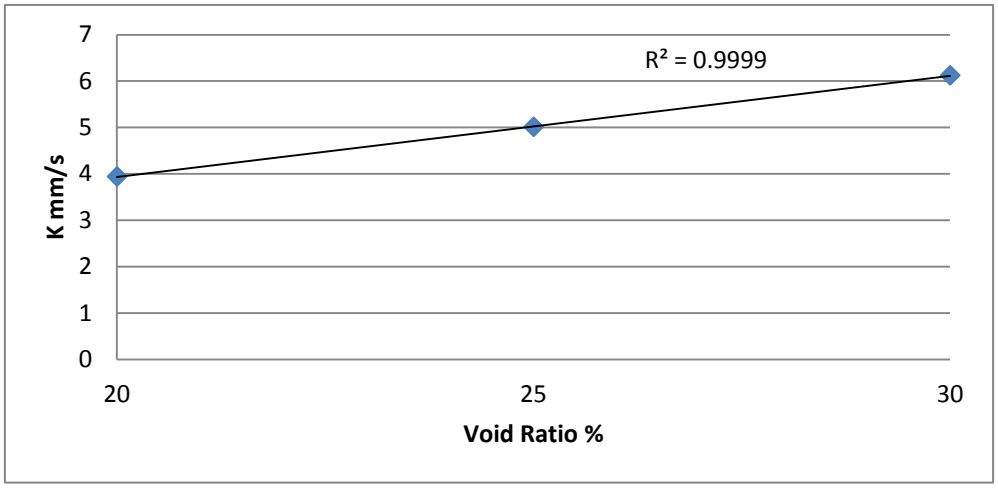

Figure 5.10 –A Constant Head Control Mixes 1, 2 and 3

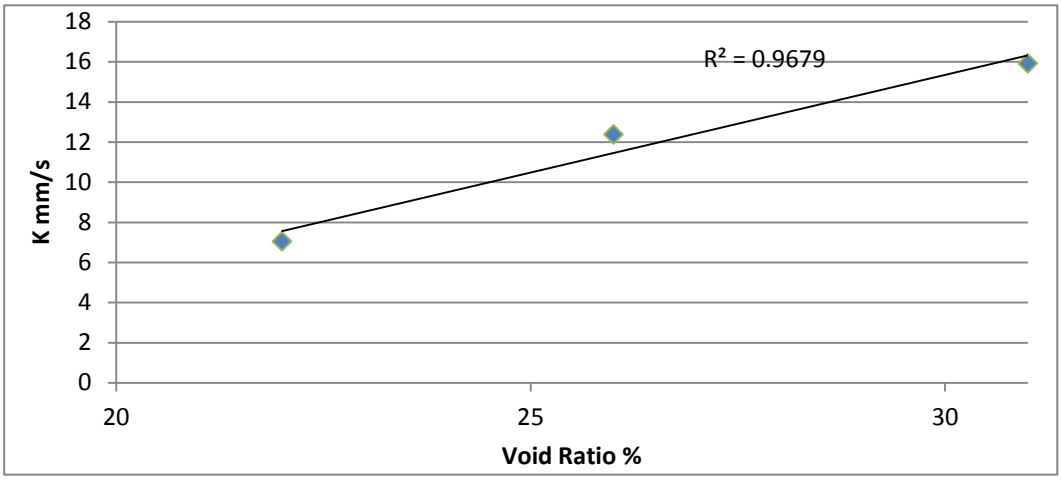

Figure 5.10 – B Falling Head Control Mixes 1, 2 and 3

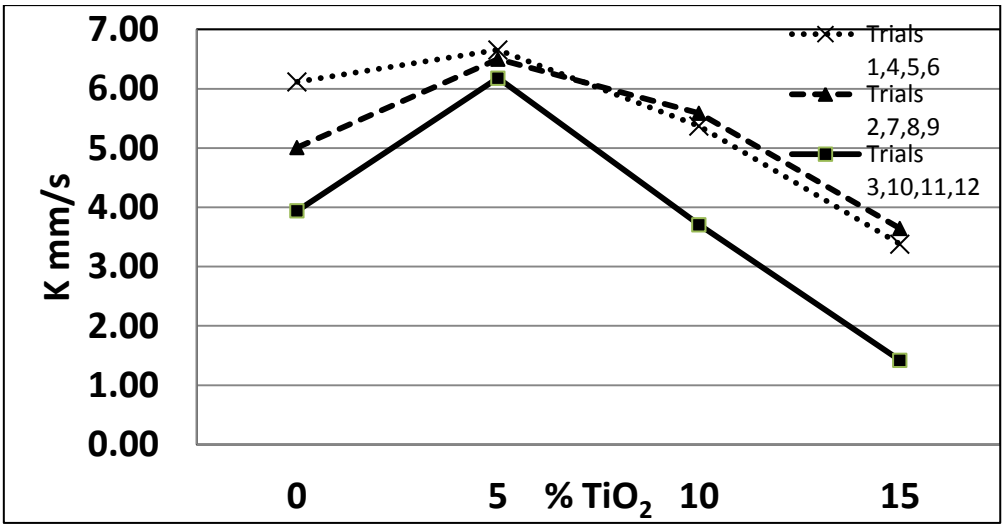

Note: Trials 1,4,5,6 orinigal mix design was 30% Void Ratio
Trials 2,7,8,9 original mix design was 25% Void Ratio
Trials 3,10,11,12 original mix design was 20% Void Ratio

Figure 5.11 Constant Head Graph

When the results were grouped in their actual void ratios, (Table 5.5 and Figure 5.12) it is apparent that there is little or no linear relationship between the addition of TiO_2 and permeability permeability. However, the result clearly show that the 15% addition of TiO_2 for all Void Ratio designs significantly reduces the permeability, in some cases greater than 50%.

Table 5.5 Normalised Constant Head Permeability Results

Trial Number Grouped	*Void Ratio %*	*0% TiO_2 (K) Falling head*	*5% TiO_2 (K) Falling head*	*10% TiO_2 (K) Falling head*	*15% TiO_2 (K) Falling head*
1,4,5,6,7,8	30	6.12	6.5	5.37	3.38
2,9,10	25	5.01	5	-	3.55
3,11,21	20	3.94	-	3.71	1.42

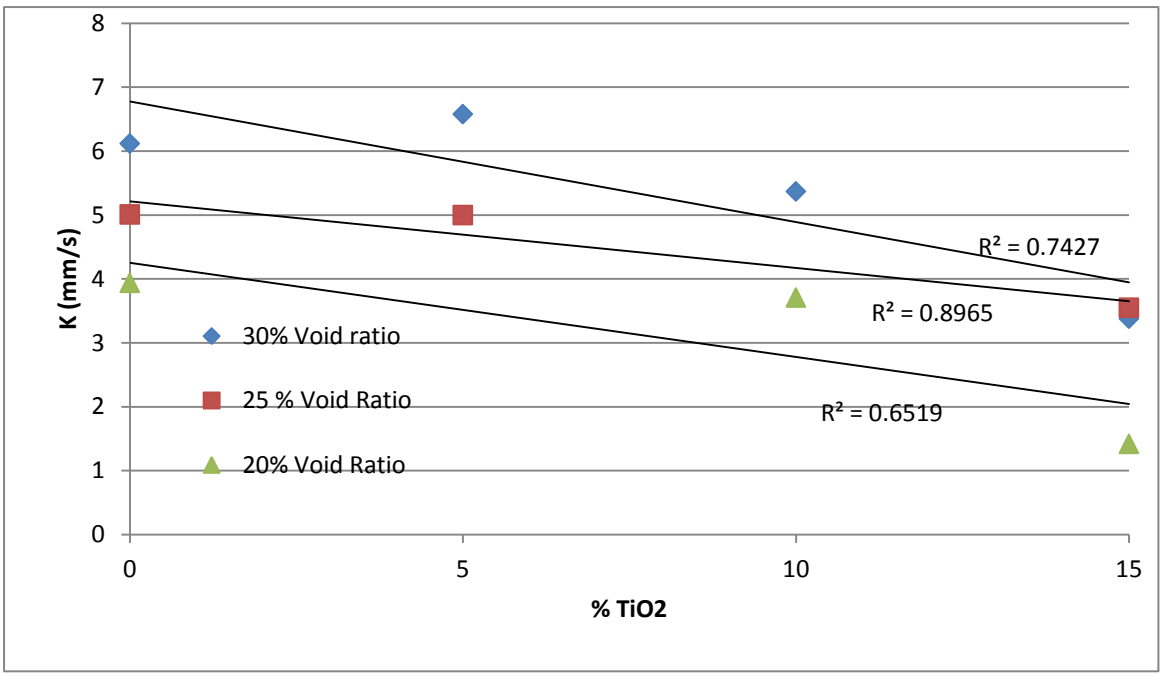

Figure 5.12 Normalised Constant Head Permeability

Although the values between the Falling Head Method and Constant Head Method are different, the trend between the two methods is the same. From the results, only the 15% addition of TiO_2 has a significant effect on the permeability.

5.3.3 Constant Head and Falling Head Comparison

The Falling Head method produced higher infiltration results than the Constant Head Method for the same samples. These findings are consistent with previous results presented by Crouch *et al* (2007), Lian, Zhuge & Beecham (2011), Parks and Tia (2004), and Zouaghi *et al* (1998).

The Falling Head and Constant Head methods are adopted from the "*Standard for measuring the permeability of soils*". In Australian Standard 1289.6.7.2 -2001 Method of Testing Soils for Engineering Purposes: Method 6.7.2: Soil Strength and Consolidation Tests – Determination of Permeability of a Soil – Falling Head Method for a Remoulded Specimen, it states that the Constant Head Method should be used instead of the Falling Head Method, for materials having a permeability greater than 10^{-7} m/s, due to excessive flow. According to the Australian Standard AS 1289.6.7.1 -2001 Method of Testing Soils for Engineering Purposes: Method 6.7.1: Soil Strength and Consolidation Tests – Determination of Permeability of a Soil – Constant Head Method for a Remoulded Specimen, this method should not be used for coefficients greater than 10^{-2} m/s due to excessive flow.

Lian, Zhuge & Beecham (2011) compared the two test methods for permeability of permeable concrete and concluded that the Constant Head Test Method was more accurate for permeable concrete tests, compared to the Falling Head Method.

The Constant Head Test is based on Darcy's Law, equation 5.1 and assumes a laminar flow for testing. Recently, Lian, Zhuge & Beecham's (2011) research applied the Reynolds' number to calculate the type of flow for each permeability test method.

Their research showed that the flow conditions were laminar. Tong's (2011), research investigated pore size and the affect it has on flow conditions. They concluded that when the pore size is greater than 0.6 cm, the flow conditions move from laminar to transitional flow. Therefore if the Reynolds number is less than 10 it is a laminar flow. Between 10 and 100 for transitional flow and >1000 for turbulent as shown in Figure 5.13. This is supported by research by Das (1997) who reported for Darcy's Law to be valid the Reynolds' number should be between 1 and 10.

$$Q = A \times K \times I \times T \quad (5.1)$$

Where:
Q = Volume of fluid
A= Cross sectional area
K = Coefficient of permeability
I = Hydraulic gradient
T = Time of measurement

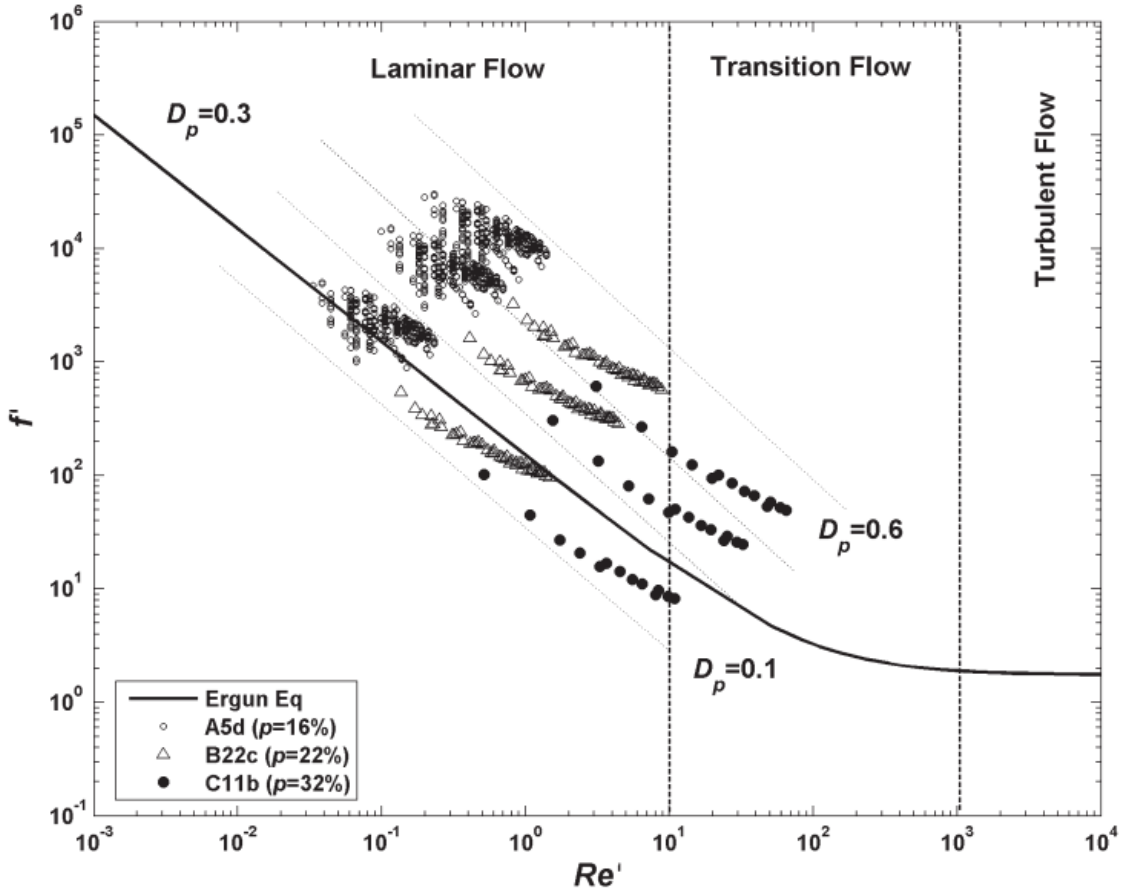

Figure 5.13 Darcy's Law Constant Head Reynolds Number (Image sourced from Tong 2011)

The pore sizes for the photocatalytic permeable concrete were generally greater than 0.6cm. These were measured from the image analysis photos, as shown in Figure 5.14.

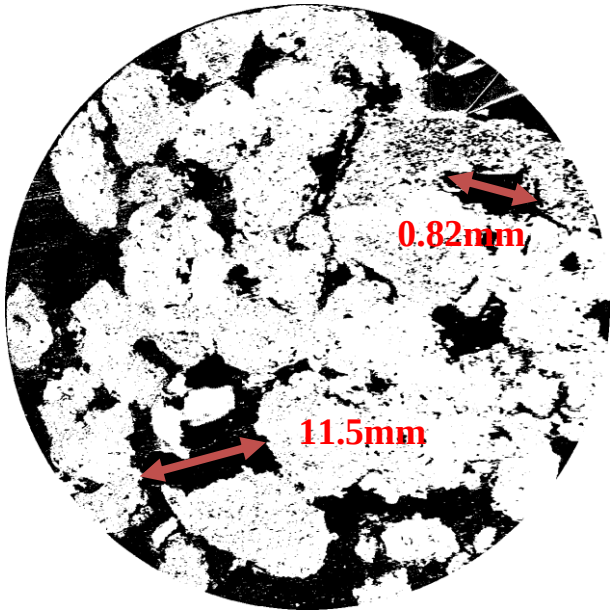

Figure 5.14. Pore Measurements Trial 10 core 3

The Reynolds' number was calculated for all the mixes applying equation 5.2. The results can be seen in Table 5.6

$$Re = \frac{pVL}{\mu} \tag{5.2}$$

Where:

V Is the mean velocity of the object relative to the fluid (m/s)
L is a characteristic linear dimension, (hydraulic diameter D_h) (m)
μ is the dynamic viscosity of the fluid (Pa·s or N·s/m² or Kg/(m·s))
ρ is the density of the fluid (Kg/m³)

Table 5.6 Reynolds' Number Calculations

Trial Number	*TiO_2 addition*	*Design Void ratio*	*Actual Void ratio*	*Reynolds Number Falling Head*	*Flow type*	*Reynolds Number Constant Head*	*Flow Type*
units	*%*	*%*	*%*	*Re*			
1	0	30	30	109.6286	Transition	42.11683	Transition
2	0	25	25	92.75818	Transition	37.53587	Transition
3	0	20	20	47.95863	Transition	26.83343	Transition
4	5	30	30	137.4241	Transition	43.48742	Transition
5	10	30	30	94.58808	Transition	32.78467	Transition
6	15	30	30	43.48337	Transition	20.15365	Transition
7	5	25	30	71.62798	Transition	39.8289	Transition
8	10	25	30	84.84275	Transition	34.43613	Transition
9	15	25	25	24.10117	Transition	25.75745	Transition
10	5	20	25	64.82935	Transition	40.08076	Transition
11	10	20	20	34.69569	Transition	26.86529	Transition
12	15	20	20	14.43614	Laminar	9.547914	laminar

The results in Table 5.6 show that almost all of the flow conditions are transition flows.

These finds are supported by Montes & Haselabach (2006) who concluded that both test methods are relatively simple and easy to set up; however the formulas show limited accuracy due to the invalid laminar flow produced by the large pore size.

The addition of TiO_2 has increased the porosity of the permeable concrete through poor compaction and therefore, the permeability. The results in table 5.6 clearly show that the Falling Head Method produced Reynolds numbers significantly higher than the Constant Head Method. Therefore, the Falling Head Method is not as appropriate for measuring the permeability of Photocatalytic Permeable Concrete. From the results the Constant Head Method appears to be more appropriate with some level of accuracy for measuring the permeability of Photocatalytic Permeable Concrete. Even though the Reynolds' results were generally greater than 10 these were at the lower end of the transition scale.

An alternative application for measuring the permeability of photocatalytic permeable concrete might be electrical impedance spectroscopy, which applies the Kozney Carmen formula, recommended by Netithalath, Weiss & Olek (2007). Currently Engineers design urban waste water management systems to be able to withhold or divert a certain amount of run-off water. The current methods for measuring permeability are not accurate for photocatalytic permeable concrete. Further research is required to determine a more accurate test method.

5.4 Compressive Strength

The compressive strength results for the control mixes Trials 1,2 and 3 ranged from 8.3MPa to 12.5MPa at 28 days. Trial 1, which had the highest design void ratio of 30%, achieved a compressive strength result of 8.3MPa. Trial 2, which had a void ratio design of 25% achieved 1.7MPa higher compressive strength results. Trial 3, with its design void ratio of 20%, achieved 4.2 MPa higher than Trial 1, as shown in Figure 5.15. A 20% strength reduction was observed between Trial 13, which had a void ratio of 0% and Trial 3 with a void ratio of 20%. Similarly, Kevern *et al* (2005) deduced that the relationship between void ratio and compressive strength was linear.

This relationship can also be seen in Figure 5.16, where the increase in void ratio had a linear reponse to the reduction in density of the concrete, producing an R^2 value of 0.998; Therefore, a relationship between density and compressive strength has been established for permeable concrete. Similarly, Sonebi & Bassuoni's (2013) research into permeable concrete mix designs found a similar relationship between density and compressive strength, with R^2 results greater than 0.96.

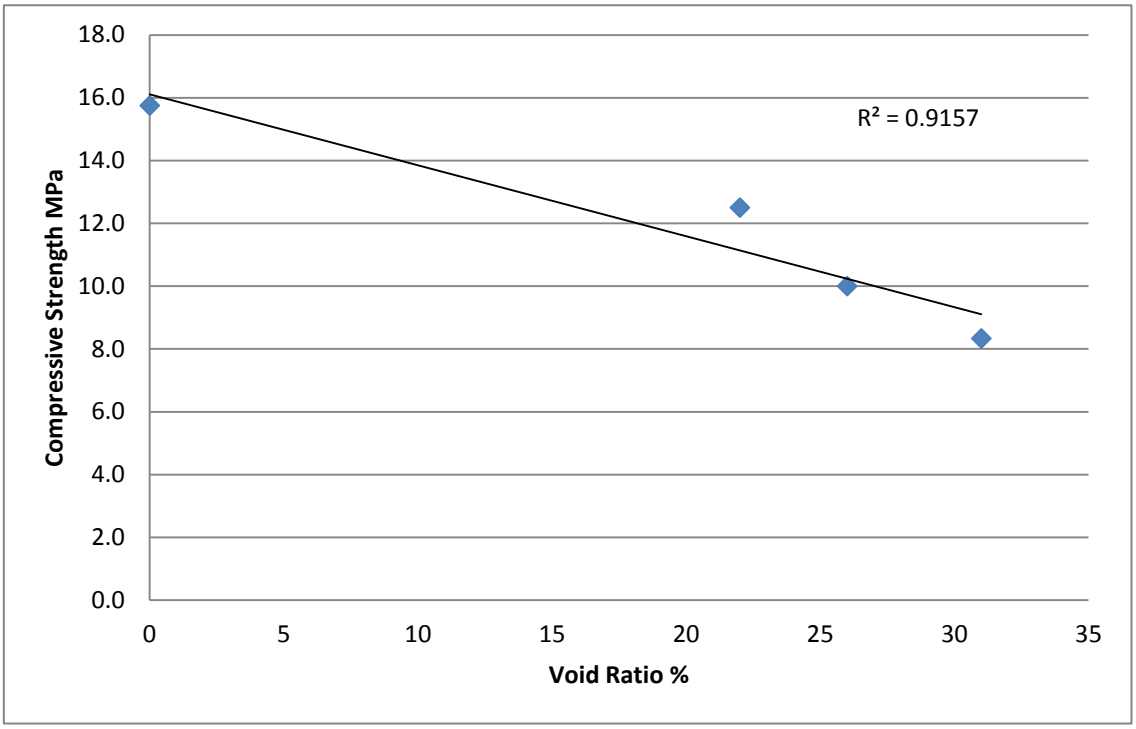

Figure 5.15 Control Mixes MPa Vs Void Ratio

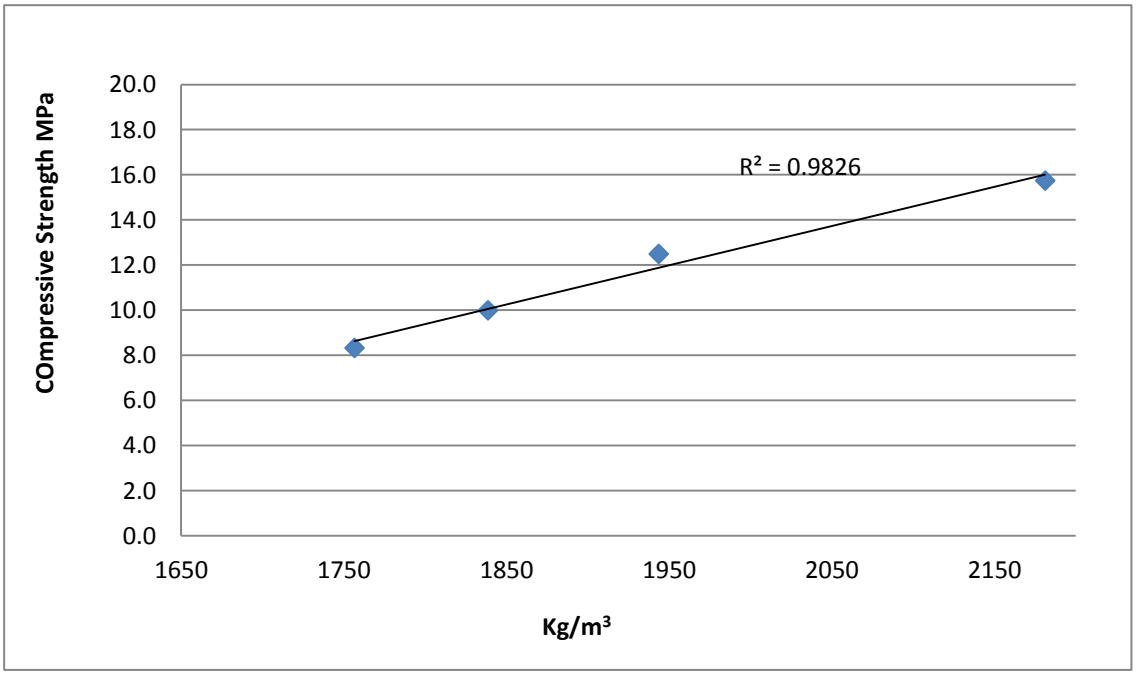

5.4.1 Void Ratio and Compressive Strength

As shown in Figure 5.17 and Table 5.1, the addition of photocatalytic TiO_2 affected the compressive strength and the density of the mixes. In general, it appears that the addition of TiO_2 increased the compressive strength and reduced the void ratio, when comparing the various additions of TiO_2. This trend of increased compressive strength with a reduction in void ratio is commonly reported for permeable concrete (Kevern *et al* 2005, Wang *et al* 2006).

However, since it has been established that the density of the permeable concrete and void ratio have a linear relationship to the compressive strength, the results have been grouped together as their actual void ratio versus compressive strength, as shown in Figure 5.18, not their designed void ratios.

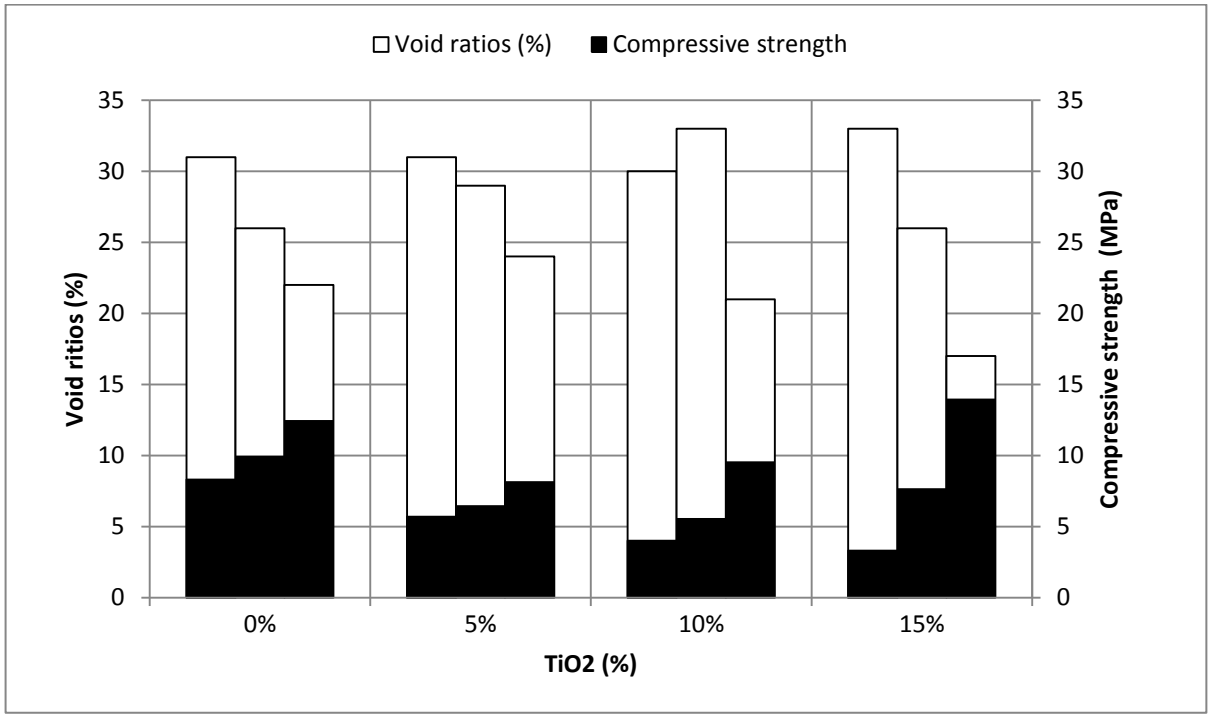

Figure 5.17 Void Ratio VS Compressive Strength – Design Void Ratio

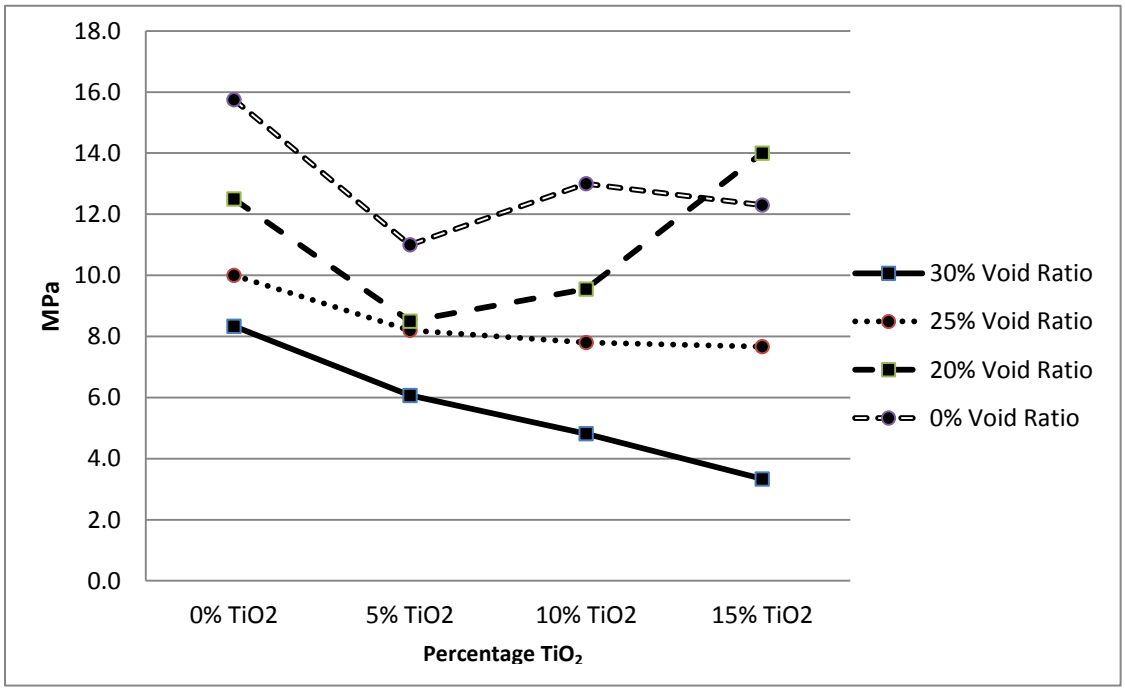

Figure 5.18 Compressive Strength VS Void Ratio – Actual Void Ratio

Figure 5.18 displays that again; a lower void ratio has higher compressive strength. However, it also demonstrated that for the higher void ratios (30 % and 25%), the addition of photocatalytic TiO_2 had a negative effect on the compressive strength, reducing the compressive strength. It appears that each 5% addition of TiO_2 reduced the compressive strength by approximately 20% for the higher void ratio mixes. However, these findings were not consistent for all void ratios. More research is required to establish the relationship between compressive strength and the addition of TiO_2 to Permeable Concrete.

These findings are not consistent with research by Lackhoff *et al* (2003), who investigated the addition of the Degussa P 25 TiO_2 to cement treated ISO prisms. They found a relative strength increase by 20%. Although Lackhoff *et al* (2003) found that the addition of TiO_2 had a pozzolanic effect on the ISO prism samples, these prisms were solid and did not contain aggregate, where as permeable concrete has large voids and contains aggregate. Therefore, they cannot be accurately compared.

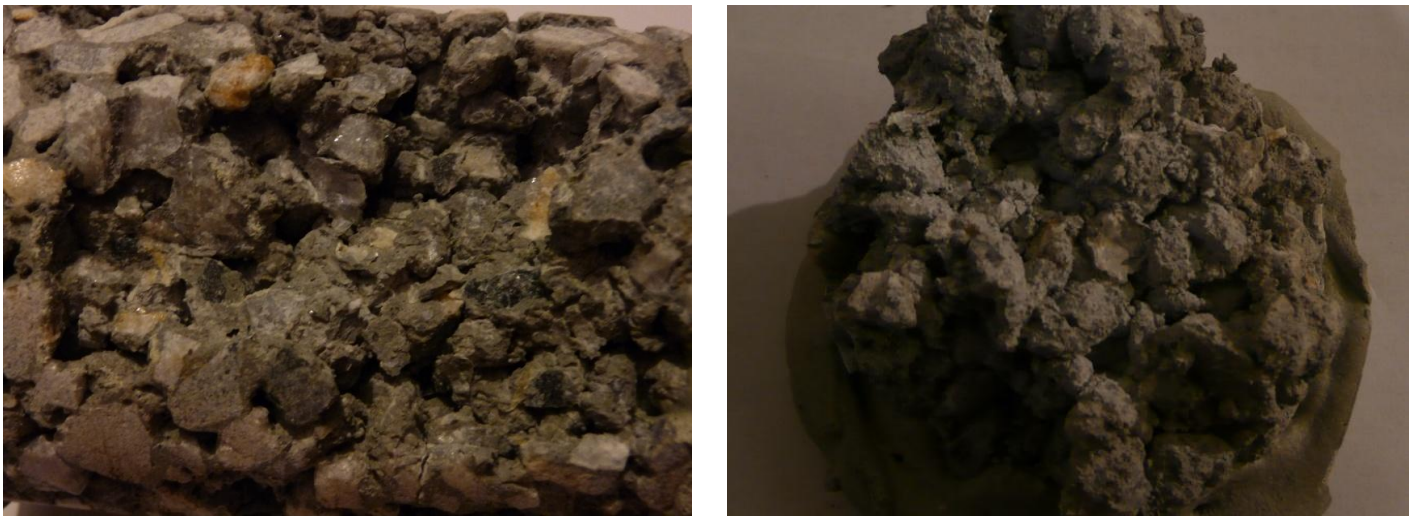

a)Trial1, 30% void ratio b) Trial 7, 30% void ratio, 10% TiO_2

Figure 5.19 Compressive Strength Testing Images

The low compressive strength results may also be explained by examining Figure 5.19a and 5.19b, which depict the fractured cores after compression testing.
The images clearly show that there has been aggregate “blow out”, which caused the low compressive strength results. These findings are also supported by the research of Chindaprasirt *et al* (2006), who reported that high void ratio mixes with low flow cement paste resulted in low compressive strength, due to the voids creating a concentration of stress, when under load.

When examining the broken cores from trials, it can be seen that the aggregate has pulled away from the paste. Therefore a reduction in strength has occurred, due to reduced aggregate bonding (Figure 5.20). Crouch *et al* (2007) concluded that an increase in aggregate quantity (void ratio) resulted in less compressive strength, as there was a reduction in cement paste for aggregate bonding.

Although the TiO_2 has pozzolanic properties it does not appear to be a 1:1 replacement for these mix designs.

The results would also suggest that additions of photocatalytic TiO_2 to permeable concrete of 10% or higher and with a void ratio greater than 25% are not recommended, due to the significant loss in strength.

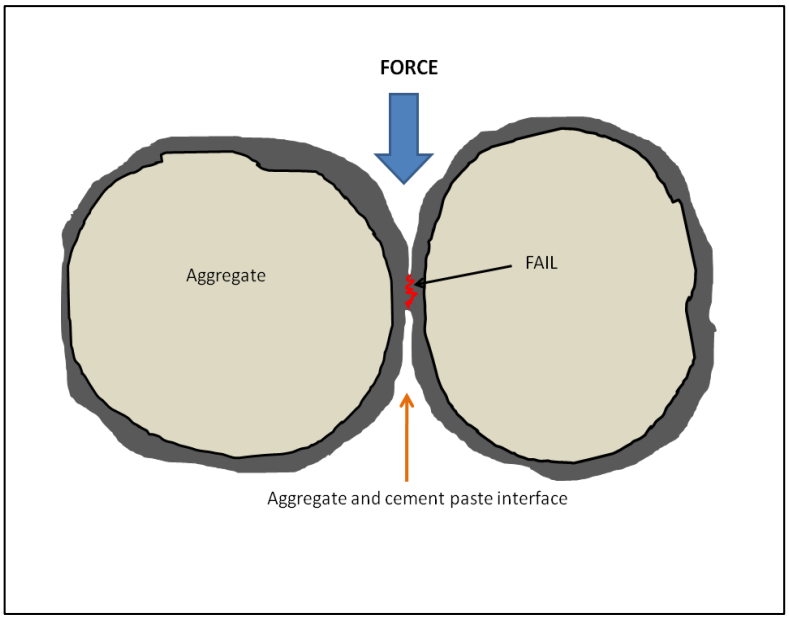

Figure 5.20 Cement Paste Aggregate Failing

6.0 Degradation of Naphthalene Results

Although the fundamental mechanisms of the photo-induced redox reaction and the super-hydrophilic conversion of TiO_2 for the degradation of organic pollutants are understood, some complex reactions are still not known (Bahnemann 2004). The reactions take place on the surface of the TiO_2, (Figure 6.1). When TiO_2 absorbs UV light (300-400nm), a photon of energy is absorbed. If the energy is equal to or greater than the TiO_2 band gap (3.2ev), this can then produce an electron/hole pair. This is caused by electrons being promoted from the valence band and being transferred to the conductive band, as expressed in Equation 6.1. The positive holes in the valence band can then react with water on the surface to produce hydroxyl radicals.

$$TiO_2 \xrightarrow{h\nu} TiO_2 + e^- + H^+ \quad (6.1)$$

$$H_2O \leftrightarrow OH^- + H^+ \quad (6.2)$$

$$OH^- + H^+ \rightarrow OH^\cdot \quad (6.3)$$

$$e^- + Ti^{4+} \rightarrow Ti^{3+} \quad (6.4)$$

$$4H^+ + 2O^{2-} \rightarrow O_2 \quad (6.5)$$

The hydroxyl radical and the electron holes have sufficient energy to oxidize organic pollutants such as aliphatic, aromatics, detergents, dyes, pesticides and herbicides (Bhatkhande *et al*. 2001).

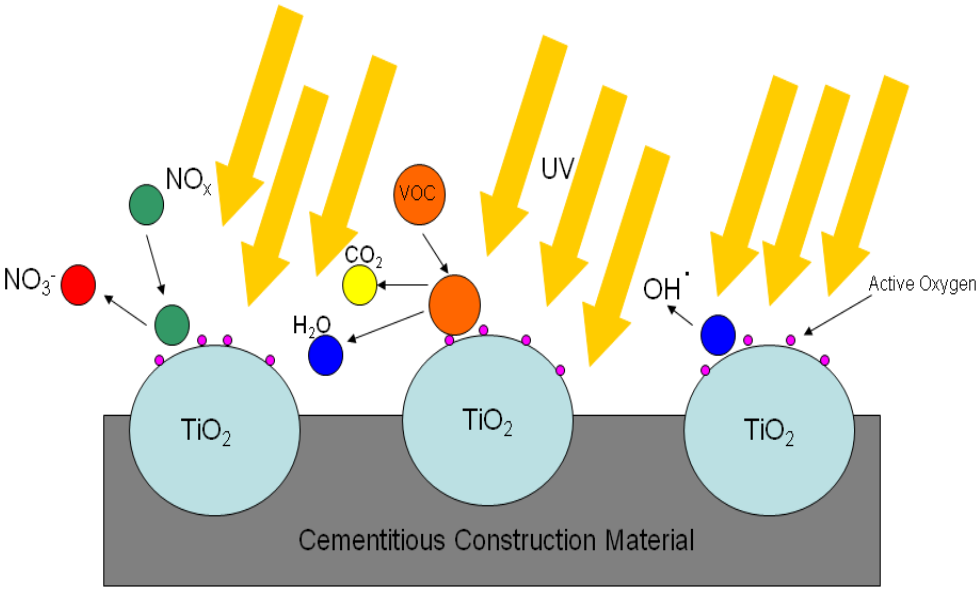

Figure 6.1 TiO_2 Construction Material Reaction Mechanisms

The degradation of Naphthalene through photocatalytic permeable concrete does not use co-solvents (acetonitrile or ethanol), or different electron acceptors (H_2O_2, $KBrO_3$) to assist the reaction rate, as these solvents would not be used in urban waste water management systems. The reaction rate was not important for this study but rather, the chemical pathway and the total percentage of degradation achieved.

When Naphthalene is degraded into simple substrates there are intermediate products formed along the reaction pathway (Lair *et al* 2008).

Once again the reaction pathway is not certain, however research by Lair *et al* (2007) and Qourzal *et al* (2007), suggests that the hydroxyl radical and the electron pair holes form these intermediates as shown in (Figure 6.2). Figure 6.3 follows the degradation pathway of 2-naphthol, an intermediate of Naphthalene, being broken down by the hydroxyl radical into intermediates until finally becoming simple substrates, CO_2 and H_2O.

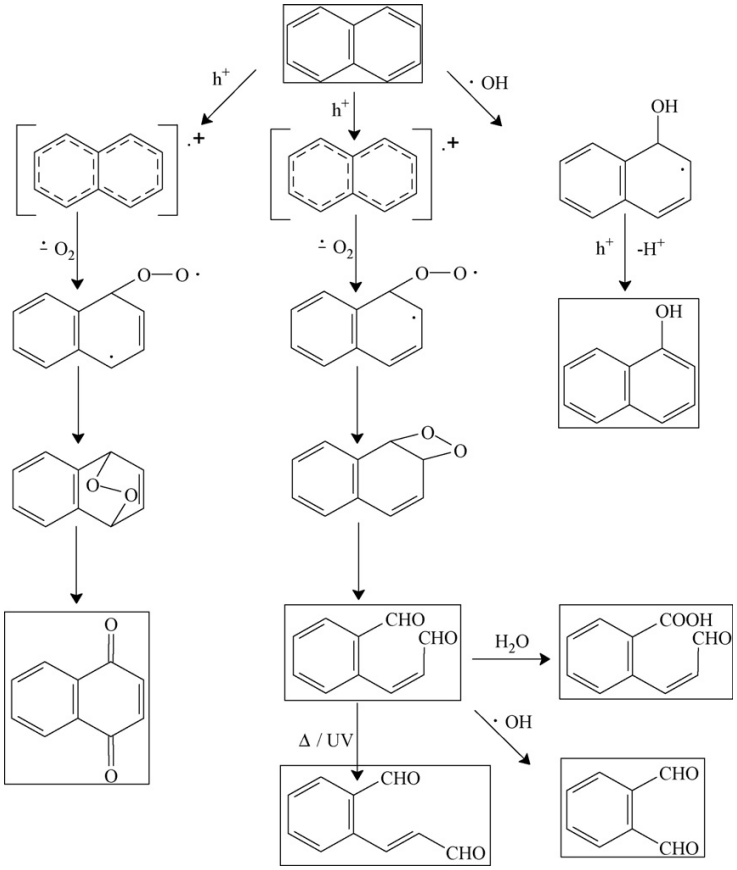

Figure 6.2 Chemical Pathway of Naphthalene Degradation (Source Lair *et al* 2007)

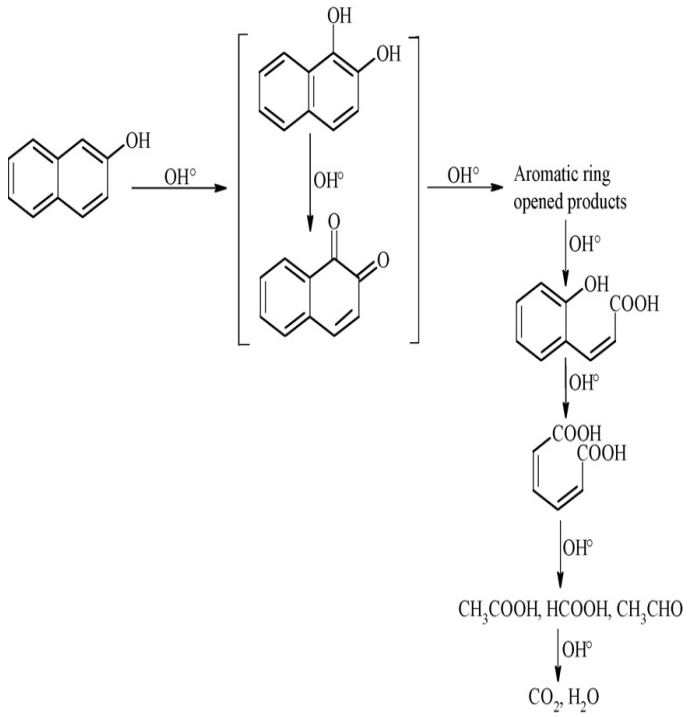

Figure 6.3 Proposed Photocatalytic Degradation Pathway of 2–naphthol (Source Qourzal *et al* 2007)

6.1 Normal Concrete – 0% Voids

The 0% void ratio concrete (Trials 13, 14, 15 and 16) was used to simulate normal structural concrete pavement and therefore, established a background for measuring whether permeable concrete is more effective for degradation than normal 0% void concrete. Four tests were conducted with 0% TiO_2, 5% TiO_2, 10% TiO_2, and 15% TiO_2 with samples taken every hour for 4 hours. The results of the degradation analysis are shown in Figure 6.4 for the first 90 minutes of testing and for 240 minutes in Figure 6.6.

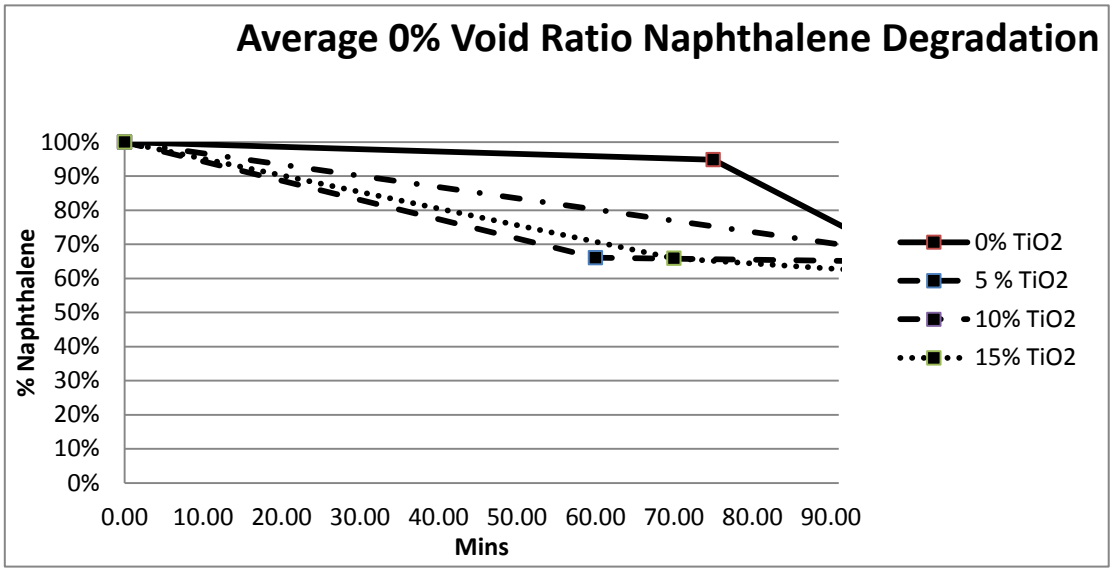

Figure 6.4 Naphthalene Degradation Over 90 Minutes 0% Void Ratio

The results for normal 0% void ratio concrete demonstrated that the addition of TiO_2 reduced the presence of Naphthalene by approximately 30% for all TiO_2 addition percentages. The sample which had no TiO_2 added (Trial 13) did not change until after 70 minutes. However, Figure 6.5 depicts that there is a significant decrease of Naphthalene at the 120 minute interval for the Trial 13.

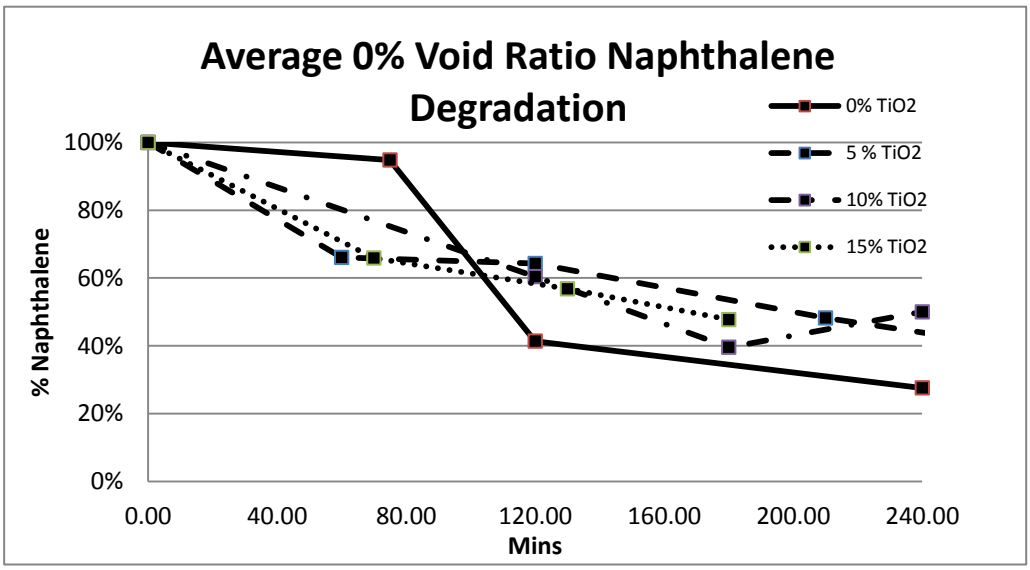

Figure 6.5 Naphthalene Degradation Over 240 Minutes 0% void ratio with various additions of TiO_2

The decrease of Naphthalene at 120 minutes for the 0% TiO_2 (Trial 13) may have been caused by the sublimation (vaporisation) of Naphthalene at temperatures greater than 308K, 35°C (Faundez *et al* 2007). At 120 minutes the temperature of the sample was 40°C. The volatility of Naphthalene could cause it to vaporize and reduce the quantity present in the water sample.

It was noted during testing that the temperature of the samples were generally higher for the 0% voids than for most of the other samples. This may have been caused by the surface of the concrete heating up under the UV lamp and not cooling as effectively as the permeable concrete samples. Nakayama & Fujita's (2010) research collaborates this theory, as their research concluded that permeable concrete has a surface temperature significantly lower than traditional concrete, due to its reduction in thermal conductivity.

The 0% void ratio, 0% TiO_2 (Trial 13) had a fluid load sample temperature generally > 4°C warmer than Trials 14, 15 and 16, (Table 6.1). The only difference was that the other trials had the TiO_2 addition.

Table 6.1 0% Void Ratio Temperature and pH Results

Trial	***Temperature***					***pH***					***TiO_2***	***TiO_2 Remaining***
Minutes	***0***	***60***	***120***	***180***	***240***	***0***	***60***	***120***	***180***	***240***	***%***	***%***
13	20.2	35	40	NT	42	5.59	10.85	10.91	NT	11.48	0	28
14	20	34	37	38.5	38	4.01	11.53	11.78	11.88	11.92	5	41
15	21	32	34	38	NT	5.05	11.1	11.68	11.71	NT	10	50
16	25	33	36	37	NT	9.81	11.19	11.2	11.29	NT	15	48

Note: NT means not tested

When TiO_2 is irradiated by UV light, the contact angle of water is reduced to almost zero over time (Takata *et al*. 2003). This means that water droplets are almost flat and spread out instead of beading up on the surface (Figure 6.6). This phenomenon is known as 'super-hydrophilicity' and may explain the lower temperatures seen in Trials 14, 15 and 16, compared to Trial 13.

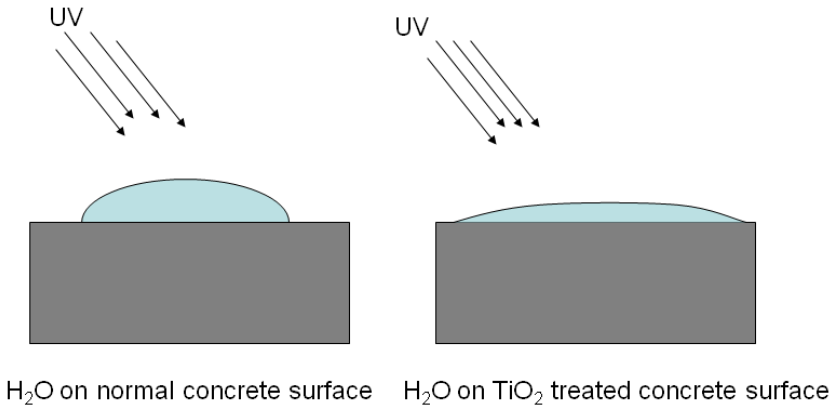

Figure 6.6 Photo-induced Super-hydrophilic Surface with Water Droplet

The super-hydrophilic reaction has three processes. First is the absorption of a photon to produce an electron/hole pair (eq. 6.1). The second is that instead of the hydroxyl and superoxide being produced, (eqs. 6.2 and 6.3), the TiO_2 surface is reduced and an oxygen vacancy is created (eq. 6.4). The third is when oxygen in the air immediately oxidizes Ti^{3+}. However, the oxygen bonds with a water molecule to form a hydroxyl group on the surface (eq. 6.5). The creation of the hydroxyl group on the surface acts as a chemisorbed water layer (Takata *et al*. 2003). When pollutants such as dirt, grit and organics come into contact with the super-hydrophilic layer, they can then be washed away with rain. There are two phenomenon involved in the degradation process. One is the photo induced redox reaction and the other is the super-hydrophilic conversion of TiO_2 that takes place on the surface of TiO_2 modified cement products, which make it a favorable method for the degradation of organic pollutants.

This phenomenon is also being used to reduce the temperature of buildings which are being cooled by the latent heat flux caused by the evaporation of the water on their surface (Chen & Poon, 2009). This cooling effect was observed in the trials (Table 6.1).

The results for the 0% TiO_2 addition can only be compared up to the 90 minute time interval, as after this the temperature is greater than 40°C and vaporisation may have occurred. It clearly shows (Figure 6.4) that before vaporisation occurs, Naphthalene does not experience degradation in normal concrete (0% voids, 0% TiO_2). Therefore, standard road, driveway and footpath pavement concrete would not experience degradation of poly-aromatic hydrocarbons under normal conditions.

Interestingly, Trial 14 which contained only the 5% addition of TiO_2, achieved the best reduction at 60 minutes (34%) and at 180 minutes (52 %). In this trial, the 15% addition of TiO_2 performed better than the 10% addition of TiO_2.

Research by Husken, Hunger and Brouwers (2009) found that increasing the surface area of the TiO_2 had a greater effect on the degradation rate of pollutants than increasing the quantity of TiO_2. Therefore, in this present study, it was expected that the three various additions of TiO_2 should produce similar degradation rates.

Although all three results are quite similar, the increased degradation seen by the 5% addition of TiO_2 could also be explained by another phenomenon; pH. Because the medium for the TiO_2 is concrete, which has a high pH, this caused all the samples to change by 5 units or more in the first 60 minutes of analysis. During the trials it was observed that Trial 16 achieved the highest pH measurements, (Table 6.1). Research by Qourzal *et al* (2008) found that a pH greater than 11 had the highest efficiency for the decomposition of 2-naphthol, which was attributed to more efficient formation of the hydroxyl radicals by the TiO_2 with increasing concentration of hydroxide ions. This increase could have been even higher but the surface of TiO_2 experiences hydration, by water being dissociated into hydroxide ions which lowers the pH by 2 units (Lair *et al* 2007).

For all the trials throughout the 240 minutes of testing, the chamber was sealed and believed to be air tight to prevent the volatile naphthalene from escaping the chamber. Further research now suggests that this may have actually hindered the total degradation of the Naphthalene (Qourzal *et al* 2008).

Figure 6.7 shows experimentation data from tests conducted by Qourzal *et al* (2008), where 2-naphthol was decomposed in a sealed chamber under normal conditions and another with the addition of O_2. The results clearly showed that the standard testing plateaus around the 90 minute time interval, when the O_2 sample continues until almost 100% degradation.

When we compare with Quorzal *et al*'s (2008) research (Figure 8.7) to Figure 6.5 there is a similar trend, with the samples plateauing and not reaching complete degradation. Although the tests of the degradation of Naphthalene in photocatalytic permeable concrete were conducted in a sealed reactor, real scale photocatalytic permeable concrete would be able to source O_2 from the surrounding atmosphere.

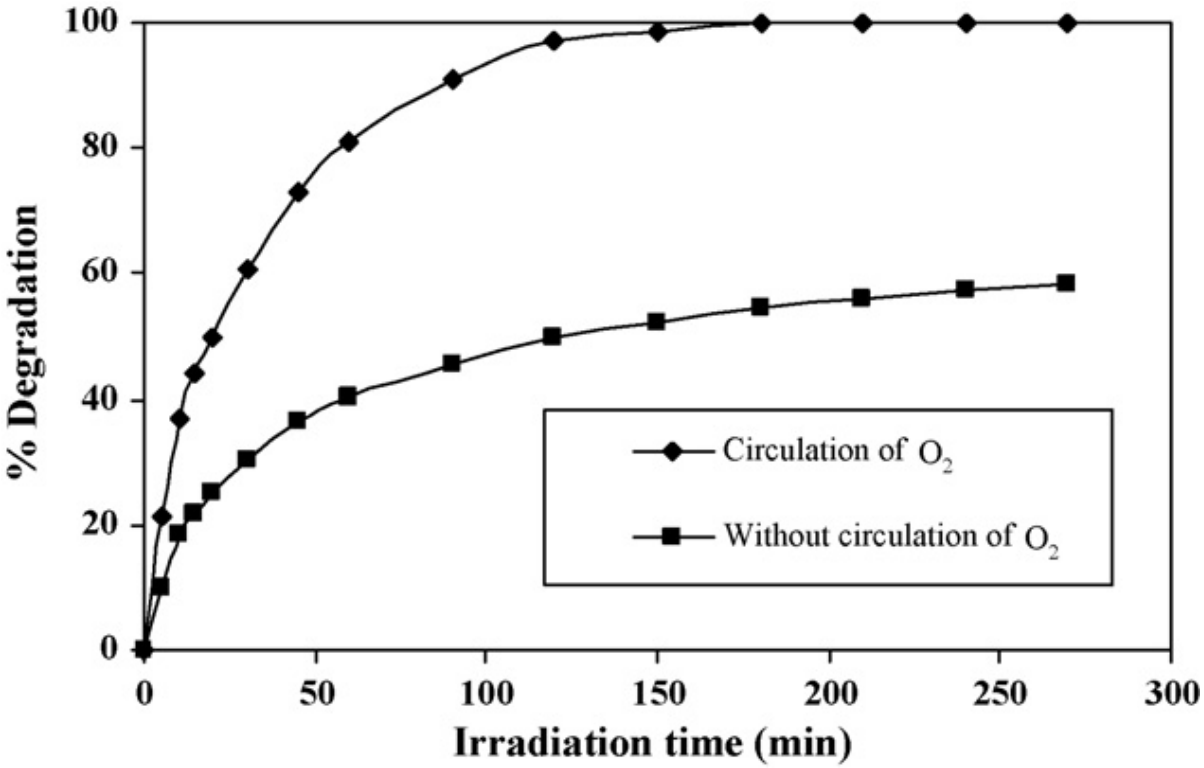

Figure 6.7 Degradation of Naphthalene in the Presence of O_2 (Sourced from Qourzal *et al* 2008)

6.2 Permeable Concrete 20% Void Ratio

The 20% void ratio degradation analysis compared 0% TiO_2, 10% TiO_2 and 15% TiO_2 additions. The 5% addition of TiO_2 was not tested, as these results were actual void ratio (as discussed previously).

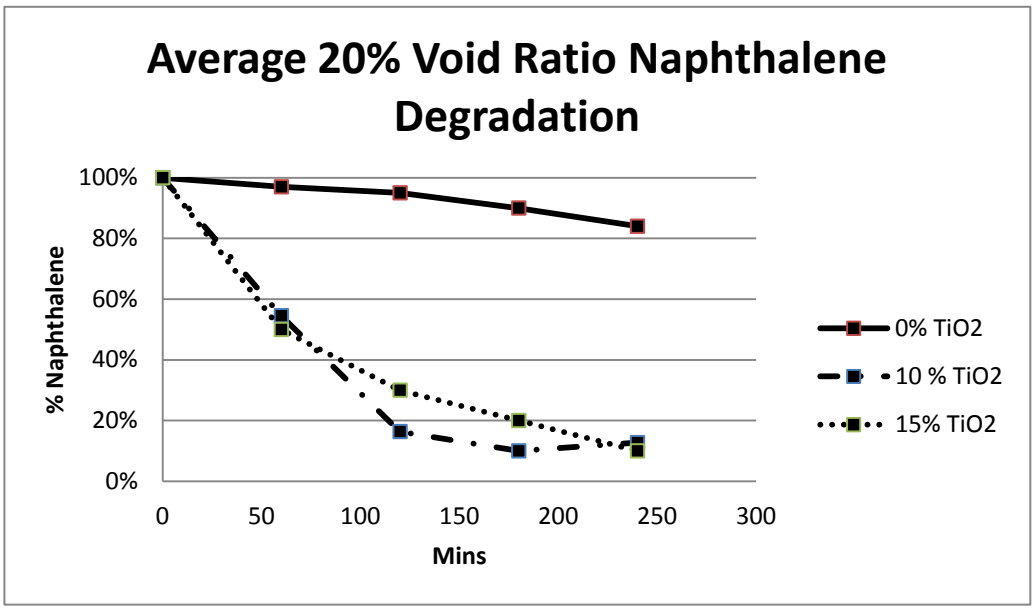

Figure 6.8 20% Void Ratio Degradation of Naphthalene

It is evident from Figure 6.8 that the two additions of TiO_2 reduced the concentration of Naphthalene significantly, compared to the control mix. The 10% and 15% addition of TiO_2 had almost identical degradation rates at 60 minutes reducing the naphthalene concentration by 50%. At the same time interval, the control mix which contained no addition of TiO_2 had a reduction of 3%. After 240 minutes of testing the 10% and 15% addition of TiO_2 samples had reduced the concentration of Naphthalene by more than 85%. The control mix at 240 minutes had reduced the concentration by 16%. However, the temperature had already achieved 35°C at 150 minutes, (Table 6.2) and any degradation would have probably been the cause of vaporisation and not the permeable concrete.

Table 6.2 20% Void Ratio temperature and pH results

Trial	***% TiO_2***	***Temperature***					***pH***				
Minutes		***0***	***60***	***120***	***180***	***240***	***0***	***60***	***120***	***180***	***240***
Trial 3	0	20.0	29.7	32.9	35.0	39.0	6.04	9.22	9.91	9.94	10.05
Trial 11	10	18.5	32.0	27.0	34.0	36.0	4.63	7.27	7.30	8.83	9.06
Trial 12	15	20.0	24.0	26.0	28.0	32.0	3.52	9.72	10.31	11.15	11.2

The 20% void ratio permeable concrete achieved the best degradation results overall, compared to the other void ratio designs.

What is interesting is that Trials 11 and 12 (10% and 15% additions of TiO_2) had some of the lowest Constant Head permeability results. It may be that as the water took longer to pass through the concrete it enabled the Naphthalene to absorb onto the surface of the concrete and oxidation occurred. Similarly, Chong *et al* (2010) reported that if there is an increase in flow of liquid past the photocatalyst, this may alter the overall photocatalytic reaction rate.

6.3 Permeable Concrete 25% Void Ratio

The degradation of Naphthalene for a 25% void ratio permeable concrete was analysed with a 5% addition of TiO_2 and a 15% addition of TiO_2. Both of these trials were compared to a control mix which had no addition of TiO_2.

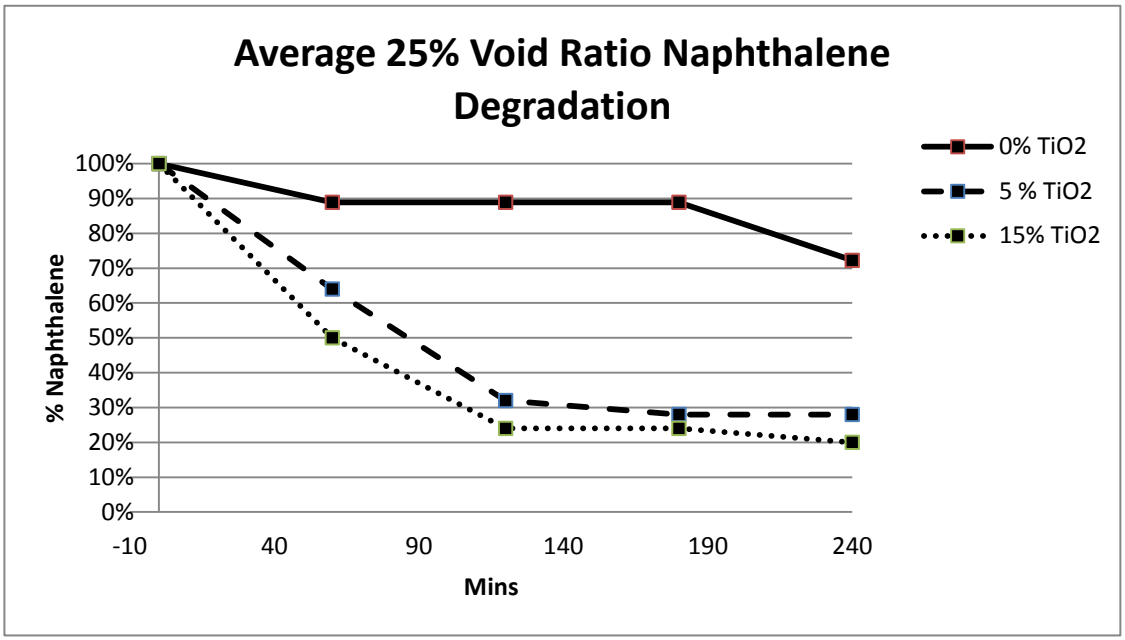

Figure 6.9 25% Void Ratio Degradation of Naphthalene

The control mix for the 25% void ratio (Trial 2) achieved 28% reduction of Naphthalene, which was the highest degradation recorded of all the control mixes. However, the temperature at 180 minutes, was greater than 35°C and hence, vaporisation may have caused the reduction in Naphthalene. Figure 6.9 reveals that the 15% addition of TiO_2 achieved slightly better results than the 5% addition, for all time intervals. The 15% addition of TiO_2 had reduced the concentration of naphthalene by 50% at 60 minutes, compared to a 34% reduction by the 5% addition of TiO_2 at 60 minutes.

However, at 240 minutes the 15% addition had reduced the concentration by 80%, which was only 8% higher than the 5% addition. This supports the previous findings in Section 6.1 and research by Hunger, Husken and Bowers (2009), where the increase in TiO_2 had less of an effect on the degradation rate than increasing the surface area.

Therefore, it would be uneconomical to add the extra 10% TiO_2 to the 25% void ratio permeable concrete for such a small gain in degradation rate.

Table 6.3 25% Void Ratio Temperature and pH Results

Trial	*% TiO_2*	*Temperature*					*pH*				
Minutes		*0*	*60*	*120*	*180*	*240*	*0*	*60*	*120*	*180*	*240*
Trial 2	0	21.0	31.0	35.0	38.5	41.0	4.80	7.27	8.25	8.87	9.30
Trial 9	15	21	28.5	32	33.5	34.5	5.61	8.89	9.04	9.12	9.88
Trial 10	5	17.7	31.0	31.5	34	35	6.97	9.36	9.68	9.83	9.96

6.4 Permeable Concrete 30% Void Ratio

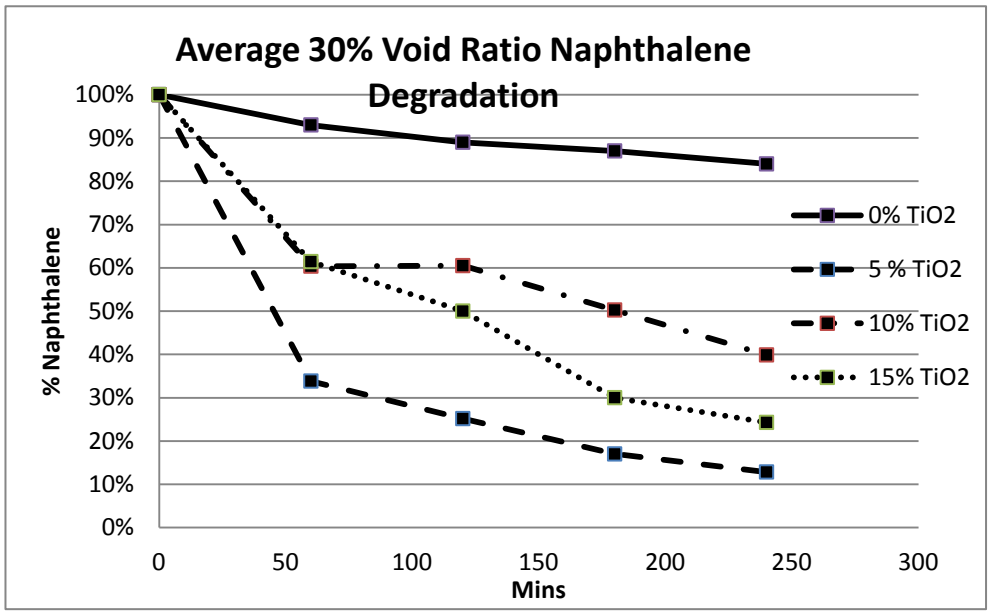

Figure 6.10 30% void ratio degradation of naphthalene

The 30% void ratio degradation results (Figure 6.10), show that the 5% addition of TiO_2 reduced the Naphthalene concentration by 87% at 240 minutes.
This result was significantly higher than the 10% TiO_2 and 15% TiO_2 addition at the same time interval. Once again this supports the conclusion that increasing the addition of TiO_2 does not increase the degradation rate.

Surprisingly, as the 30% void ratio had the largest surface area, it was expected that it would have the highest degradation rate. The 5% and 10% addition of TiO_2 results are very similar to the other void ratio results with the same quantity of TiO_2. However, when comparing the 30% void ratio degradation results to the other void ratios, it is clear that the 30% void ratio with 15% TiO_2 did not perform as well as the other void ratios with 15% TiO_2 addition. It was noted previously that the 30% void ratio permeable concrete achieved the highest rate of permeability for both permeability test methods. The reduction in degradation may have been caused by the increase rate of fluid flow through the permeable concrete, which reduced the H_2O contact time with the H^+ ions present on the surface of photocatalytic concrete and therefore, reduced the formation of the hydroxyl radicals.

Another explanation could be, although, it has a higher void ratio it does not necessarily provide a better opportunity for photocatalysis, as there is no reason that light would penetrate significantly more deeply into the porous structure.

Therefore, the research has demonstrated that the 20% void ratio photocatalytic permeable concrete was most effective for the degradation of poly aromatic hydrocarbons present in water samples.

7.0 Conclusion

The purpose of this research was to ascertain whether photocatalytic permeable concrete was more effective in the degradation of organic pollutants than traditional concrete pavement. The addition of photocatalytic TiO_2 to permeable concrete was fundamental to this research. However, little was known about the effects that it would have on the hydraulic and mechanical properties. By undertaking this research it was hoped that it would add to the existing body of knowledge on photocatalytic construction materials and increase awareness of alternative urban waste water treatments systems and the understanding of permeable pavement systems.

The information gathered in this research has provided extensive knowledge as to the ideal mix design characteristics for maintaining desired mechanical and hydraulic properties, whilst achieving a cost effective degradation of poly aromatic hydrocarbon pollutants in road runoff water. The major conclusions of this research are discussed in the following sections.

7.1 Mechanical Properties

The interconnecting voids in permeable concrete distinguish it from normal concrete pavement. It is well documented that the voids present in permeable concrete have an effect on the mechanical and hydraulic properties. However, little was known about the effect of the addition of photocatalytic TiO_2 on these properties. This research will be able to be applied by the industry, to improve these properties for potential future work.

Because the void ratio of the permeable concrete is critical to the hydraulic and mechanical properties, it was important to establish an accurate analysis of the void ratio percentage. Two alternative methods were used to analyse the void ratio; the standard void ratio and the image analysis method. The research demonstrated that the image analysis method was slightly more accurate as it was able to measure dead end pores, which may have had air bubbles trapped inside. However, the Standard Test Method is the preferred test method for measuring the void ratio for photocatalytic permeable concrete, as it is relatively fast with an accepted level of accuracy.

The results in Section 3.2 demonstrate that the addition of TiO_2 increased the void ratio of the permeable concrete. The void ratio is a function of mix design and effective compaction. The addition of photocatalytic TiO_2 significantly reduced the workability of the concrete and therefore the compaction of the permeable concrete, when being cast. This in turn increased the void ratio of the permeable concrete.

Standard concrete pavement is designed to have a compressive strength of 20MPa or greater. The interconnecting voids that make up permeable concrete significantly reduced the compressive strength as the aggregate paste bond is weak. This causes failing. It is also well documented that there is a relationship between compressive strength and void ratio. This relationship was noted in the research for the control mixes and the TiO_2 addition mixes and therefore, made it easy to be able to predict compressive strengths of photocatalytic permeable concrete with various design void ratios.

The compressive strength results showed that the addition of photocatalytic TiO_2 reduced the compressive strength by up to 20%. This was caused by the reduction in aggregate-cement paste bonding. The research indicated that permeable concrete with void ratios greater than 25% and with additions of photocatalytic TiO_2 greater than 10% recorded the highest loss in strength. From the trials, the 20% void ratio with 5% addition of TiO_2 appears to be the most effective concrete design, as it achieved little loss in strength and relatively low cost.

7.2 Hydraulic Properties

Recently, the Falling Head Method has been questioned by researchers, for its accuracy in testing the permeability of permeable concrete. Research by Lian Zhuge & Beecham (2011) showed that the Constant Head Method was more accurate for testing the permeability of permeable concrete than the Falling Head Method. The two test methods were compared for this research to determine if the TiO_2 had any effect on the permeability and to ascertain which method is more appropriate for photocatalytic permeable concrete.

Both test methods showed that increasing the addition of TiO_2 reduced the permeability of the concrete by up to 50%.
Although both test methods produced a similar trend, the Falling Head Methods produced a significantly higher result, which was also observed by previous researchers. Therefore, the 5% addition of TiO_2 has proven to be the most suitable dose rate for permeability of photocatalytic permeable concrete.

Further research in this study applied the Reynolds' number to calculate the type of flow and therefore concluded which test method would be most accurate of photocatalytic permeable concrete. The results concluded that almost all the flows produced by the photocatalytic permeable concrete were transitional flow. Therefore it can be concluded that both test methods are inaccurate for testing photocatalytic permeable concrete to measure k (k is permeability flow rate).

7.3 Degradation of Naphthalene

The use of photocatalytic permeable concrete in urban environments for waste water management systems creates a unique approach to the harnessing and detoxification of urban runoff waters. Recently, photocatalytic TiO_2 had been applied into construction materials for the degradation of organic pollutants in air and for self cleaning properties. However, little or no research had been conducted on the application of photocatalytic permeable concrete and the degradation of organic pollutants in water.

From observing the control mixes which did not contain any TiO_2, it can be concluded, that standard road, driveway and footpath concrete pavement would not undergo degradation of poly-aromatic hydrocarbons under normal conditions. Standard concrete pavement containing TiO_2 will undergo degradation of a poly-aromatic hydrocarbon and reduce the concentration by up to 55% in 240 minutes. The results for the standard photocatalytic concrete showed that increasing the dose rate of TiO_2 had very little effect on the degradation rate.

The photocatalytic permeable concrete significantly reduced the concentration of the poly-aromatic hydrocarbon for all three void ratios. The photocatalytic permeable concrete achieved 30% higher reduction than the photocatalytic standard concrete.
Similarly, the increased dose rate of TiO_2 had little effect on the overall degradation or rate of the polyaromatic hydrocarbon. This therefore, showed that photocatalytic permeable concrete is superior for the degradation of organic compounds, compared to standard photocatalytic concrete. This is due to the increased surface area created by the void allowing more reaction sites on the surface of the concrete. The different void ratios produced varying results. The 20% void ratio was the most effective, due to the reduction in permeability, which allowed more time for the reaction to take place.

7.4 Summary

This research has demonstrated that photocatalytic permeable concrete could be an ideal alternative to low strength traditional pavement systems in urban environments, for the incorporation with waste water management systems. A baseline was established to determine the effect that the addition of TiO_2 had on the permeable concrete. It was demonstrated during the laboratory trials due to its particle size and density, that the addition of TiO_2 significantly reduced the workability and therefore compaction of the Photocatalytic Permeable Concrete. This can be overcome by increasing the water cement ratio with no discernible reduction in compressive strength. An addition of 5% TiO_2 has shown to have the least effect on the mechanical and hydraulic properties of the concrete. Moreover, it also appears to be the most effective dose rate for the degradation of organic pollutants and has with minimal cost additions to the overall mix design. From the research it can be concluded that a 20% void ratio design is most effective mix design for mechanical and hydraulic properties but most importantly for the degredation of poly-aromatic hydrocarbons present in simulated road runoff.

8.0 Recommendations

There are several key areas of recommendation from this research, which can be applied to future studies into photocatalytic permeable concrete or which can be used practically in the field to produce photocatalytic permeable concrete.

8.1 Chemical Admixtures

Chemical admixtures aid in improving the concrete properties in the wet and hardened state. During the trials it was observed that insufficient compaction was achieved, due to the poor rheology of the low water cement ratio of permeable concrete. The use of chemical Polycarboxylic Ether (PCE) plasticisers and Viscosity Modifying Admixtures (VMA) would hopefully improve the compaction of the concrete and therefore the compressive strength, permeability and void ratio.

8.2 Degradation Analysis

There was little or no research on the application of photocatalytic permeable concrete being used for the purification of water and even less information available on reactors to test this application. The photocatalytic reactor was designed from other photocatalytic applications. However, future studies into photocatayltic permeable concrete should make several adjustments to the apparatus to improve the degradation of the PAH. Firstly, it should be equipped with a temperature controlled cooling jacket. This will ensure that even when the concrete medium heats up it will not go greater than 35°C and potentially cause vaporisation to occur. Secondly, the apparatus should be equipped with an O_2 sensor and O_2 gas inlet. In this way the degradation rate could be followed by measuring the O_2 decrease and then replenished by the gas inlet to ensure the reaction reaches completion. Such refinement is beyond the current scope of this research and should be investigated by future researchers.

8.3 Simulated Pavement

The reticulation system used in this research was designed to gain an understanding of photocatalytic permeable concrete and to ascertain whether it could be applicable for real life concrete pavement systems.
The next step is to test photocatalytic permeable concrete as a simulated pavement with a granular subbase, rock subbabse and soil subbase. The fluid load samples could be taken from each layer to determine the overall effectiveness. The impact of the structural layers would need to be taken into account as they would have an effect on the overall permeability of the system. This research is beyond the current investigation and should be undertaken in later studies.

8.4 Permeability

The research indicated that the Falling Head Method is not accurate for measuring the permeability of Photocatalytic Permeable Concrete. Although, the Constant Head Method has shown to have some level of accuracy for measuring the permeability, engineers and researchers would both benefit from further investigations into both the limitations of the current method and of alternative methods for measuring the permeability of photocatalytic permeable concrete. One of the second level objectives of this research was to establish which method was more appropriate to measure permeability for photocatalytic permeable concrete; the Falling Head or the Constant Head. Therefore, any further research into alternative test methods is beyond the scope of the project and the existing methods sufficed at this stage.

8.5 Incorporating light-Penetrating Technologies

Recently, studies by Chen and Poon (2011) have incorporated recycled glass into their photocatalytic concrete to increase the degradation rate. Further studies could be done incorporating light-penetrating technologies such as glass aggregates or glass fibres to increase the performance of TiO_2 embedded deeper in the permeable concrete.

9.0 References

Aamer, M, Tsuruta, K, Miriza, J 2012, 'Evaluation of high-performance porous concrete properties', *Construction and Building Materials,* Vol.31, PP. 67-73

Australian Standard, 1012.3.1 - 1998 , Methods of testing concrete – Determination of properties related to the consistency of concrete – Slump test

Australian Standard, 1012.1 -1993 Methods of testing concrete – Sampling of fresh concrete

Australian Standard 1012.12.2 -1998, Methods of testing concrete – Determination of mass per unit volume of hardened concrete – Water displacement

Australian Standard 1012.14 -1991, Methods of testing concrete – Method of securing and testing cores of hardened concrete for compressive strength.

Australian Standard 1012.2 -1994, Methods of testing concrete – Preparation of concrete mixes in the laboratory

Australian Standard 1012.3.1 -1998, Methods of testing concrete – Determination of properties related to the consistency of concrete – Slump test

Australian Standard 1012.3.2 -1998, Methods of testing concrete – Determination of properties related to the consistency of concrete – Compacting factor test

Australian Standard 1012.9 -1999- Method of Testing Concrete – Determination of Compressive Strength of Concrete Specimens

Australian Standards; Australian Standard 1012.12.1- 1998- Method for Testing Concrete - Determination of Mass Per Unit Volume of Hardened Concrete – Rapid Measuring Method

Australian Standard AS 1012.14-1991- Method for Testing Concrete – Method for Securing and Testing Cores from Hardened Concrete for Compressive Strength.

Australian Standard 1289.6.7 -2001, Methods of testing soils for engineering purposes – Soil strength and consolidation tests –Determination of permeability of a soil

Australian Standard AS 1289.6.7.1 -2001 Method of Testing Soils for Engineering Purposes: Method 6.7.1: Soil Strength and Consolidation Tests – Determination of Permeability of a Soil – Constant Head Method for a Remoulded Specimen

Australian Standard 1289.6.7.2 -2001 Method of Testing Soils for Engineering Purposes: Method 6.7.2: Soil Strength and Consolidation Tests – Determination of Permeability of a Soil – Falling Head Method for a Remoulded Specimen

Australian Standard 1478.1 -2000, Chemical admixtures for concrete, mortar and grout admixtures for concrete

Australian Standard, 2269 -2004, Plywood – Structural

Australian Standard 3582.1 -1998 Supplementary Cementitous Material for use with Portland and Blended Cement – Part 1: Flyash

Australian Standard 3972 -2010 General Purpose and Blended Cements.

Australian Standard, 6669 -2007, Plywood – Formwork

Bahnemann, D 2004, 'Photocatalytic water treatment: Solar energy applications', *Solar Energy*, vol. 77, pp. 445 - 59.

Bhatkhande, D, VPangarkar, V, Beenackers, A 2001, 'Photocatalytic degredation for environmental applications – a review', *Journal of Chemical Technol Biotechnol*, vol. 77, pp. 102-106.

Carey, J, Lawrence, J, Tosine, H 1976, 'Photodechlorination of PCB's in the presence of titanium dioxide in aqueous suspensions', *Bull. Environ. Contam. Toxicol*. vol .16, pp. 697 – 701

Chen, J, Poon, C 2009, 'Photocatalytic construction and building materials: From fundamentals to applications', *Building and Environment*, vol. 44, pp. 1899 - 906.

Chen, J, Poon, C 2011, 'Photocatalytic activity of titanium dioxide modified concrete materials – influence of utilizing recycled glass cutlets as aggregates', *Journal of Environmental Management*, vol. 90, 3436-42

Chindaprasirt, P, Hatanaka, S, Chareerat, T, Mishima, N & Yuasa, Y 2006, 'Cement paste characteristics and porous concrete properties', *Construction and Building materials*, vol. 22, pp. 894 - 901.

Chong, M, Jin, B, Chow, C, Saint, C 2010, 'Recent developments in photocatalytic water treatment technology: A review', *Water Research*, vol. 44, pp. 2997 -3027

Coleman, H, Vimonses, V, Leslie, G, Amal, R 2007, 'Removal of Contaminants of Concern in Water Using Advanced Oxidation Techniques', *Water Science & technology,* vol. 55, pp 301 - 306

Crouch, L, Pitt, J & Hewitt, R 2007, 'Aggregate effects on pervious Portland cement concrete static modulus of elasticity', *Materials in Civil Engineering*, vol. 19, No. 7, pp 561 – 68.

Das, B, 1997 'Advanced Soil Mechanics, Second Edition', Taylor and Francis, Washington DC,

Deo, O, Neithalath, N 2011, 'Compressive response of pervious concretes proportioned for desired porosities', *Construction and Building Materials*, vol. 25, pp. 4181-4189

Doll, T, Frimmel, F 2004, 'Development of Easy and Reproducible Immobilization Techniques Using TiO for Photocatalytic Degradation of Aquatic Pollutants', *Acta hydrochem.hydrobiol*, vol. 32, pp 201-13

Eriksson, E, Baun, A, Scholes, L, Ledin, A, Ahlman, A, Revitt, M, Noutsopoulos, C, Mikkelsen, P 2006, 'Selected stormwater priority pollutants – a European Perspective', *Science of the total environment*, vol. 383, pp 41 – 51

Faundez, C, Valdes, J, Valderrama, J 2007, 'Determining sublimation pressures from solubility data of solids in different solvents', *Thermochimica Acta*, vol. 462, pp. 25 – 31

Fortes, R, Merighi, J & Bandeira,A, 'Laboratory Studies on performance of Porous Concrete', *Google Scholar view 25th June 2009,* <http://meusite.mackenzie.com.br/rmfortes/publicacoes/belqcp.pdf>

Gilbert, JC, J 2006, 'Stormwater runoff quality and quantity from asphalt, paver, and crushed stone driveways in Connecticut', *Water Research*, vol. 40, pp. 826 - 32.
Haselbach, L, Valavala, S & Montes F 2006, 'Permeability prediction of sand-clogged Portland cement pervious concrete pavement systems', *Environmental Management*, vol. 81, pp. 42 - 9.

Gobel, P, Dierkes, C, Coldeway, W 2006, 'Storm water runoff concerntration matrix for urban run areas', *Journal of contaminant hydrology*, Vol. 91, pp. 26 – 42

Haselbach, L, Valavala, S, Montes, F 2006, 'Permeability prediction of sand-clogged Portland cement pervious concrete pavement systems', *Environmental Management*, vol. 81, pp 42 - 49.

Husken, G, Hunger, M, & Brouwers, H.J.H 2009, 'Experimental study of photocatalytic concrete products for air purification', *Building and Environment*, pp. 1 -12.

Kevern, J, Wang, K, Suleiman, M, & Schaefer, V 2005, '*Mix Design Development for Pervious Concrete in Cold Weather*', *Concrete Technology Forum,* NRMCA, May 24-5th 2006, Nashville, TN

Kwiatkowski, M, Welker, A, Traver, R, Vanacore, M & Ladd, T 2007, 'Evaluation of an infiltration best management practice utilizing pervious concrete', *The American water resources association*, vol. 43, no. 5, pp. 1208- 22.

Lackhoff, M, Prieto X, Nestle, N, Dehn, F & Niessner, R 2003, 'Photocatalytic activity of semiconductor-modified cement - influence of semiconductor type and cement ageing', *Applied catalysts*, vol. 43, pp. 205 – 16

Lair, A, Ferronato, C, Chovelon, J, Herrmann, J, 2007, 'Naphthalene degradation in water by heterogeneous photo catalysis: An investigation of the influence of organic ions,' *Journal of photochemistry and photobiology*, vol.193, pp. 193 – 203

Lian, C, Zhuge, Y 2010, 'Optimum mix design of enhanced permeable concrete – An experimental investigation", Journal of Construction and Building Materials, vol 24, 2664–2671.

Lian, C, Zhuge, Y, Beecham, S 2011, 'Evaluation of permeability of porous concrete', *Journal of Advanced Materials Research*, Vols. 295-297, 873-879.

Luck, J, Workman, S, Coyne, M & Higgins, S 2008, 'Solid material retention and nutrient reduction properties of pervious concrete mixtures', *Biosystems Engineering*, vol. 100, pp. 401- 8.

Luck, J, Workman, S, Coyne, M & Higgins, S 2009, 'Consequences of manure filtration through pervious concrete during simulated rainfall events', *Biosystems Engineering*, vol. 102, pp. 417 - 23.

Marlof, A, Neithalath, N, Sell, E, Weiss, J & Olek, J 2004, 'Influence of aggregate size and gradation on the acoustic absorption of enhanced porosity concrete', *American Concrete Institute*, vol. 101, no. 1, pp. 82 - 91.

Montes, F, Haselbach, L 2006, 'Measuring Hydraulic Conductivity in Pervious Concrete', Environmental Engineering Science, Volume 23, Number 6.

Nakayama, T, Fujita, T 2010, 'Cooling effect of water-holding pavements made of new materials on water and heat budgets in urban areas', *Landscape and urban planning*, vol. 96, pp. 57 -57

Neithalath, N, Weiss, J & Olek, J 'Acoustic Absorption Behaviour of Fiber Reinforced Enhanced Porosity Concrete'. Google Scholar, viewed 15th June 2009, <http://cobweb.ecn.purdue.edu/~concrete/weiss/publications/o_conference/OC-018.pdf>

Neithalath, N, Weiss, J & Olek, J 'Predicting the Permeability of Pervious Concrete (enhanced Porosity Concrete) from Non-Destructive Electrical Measurements', Google Scholar viewed 30th June 2009, <https://fp.auburn.edu/heinmic/PerviousConcrete/Porosity.pdf>

Park, S, & Tia, M 2003, 'An experimental study on water-purification properties of porous concrete', *Cement and Concrete Research*, vol. 34, pp. 177 - 84.

Putman, B, Neptune, A 2011, 'Comparison of test specimen preparation techniques for pervious concrete pavements', Construction and Building Materials, Vol. 25, pp. 3480 -3485

Qourzal, S, Barka, N, Tamimi, A, Assabbane, Y, Ait-Ichou, Y 2008, 'Photodegrdation of 2-naphthol in water by artificial light illumination by TiO_2 photocatalyst: Identification of intermediates and the reaction pathway', *Applied Catalysis* , Vol. 33, pp. 386 – 393

Safiuddin, M, Hearn, N 2005, 'Comparison of ASTM saturation techniques for measuring the permeable porosity of concrete', *Cement and Concrete Research*, vol. 35, pp. 1008 - 13.

Sanchz & Sobolev 2010, 'Nano Technology in Concrete – A review', *Construction and Building Material*s, vol. 24, pp. 2060-2071

Schipper, P, Comans, R, Dikstra, J & Vergouwen,L 2007, 'Run off and windblown vehicle spray from road surfaces, risks and measures for soil and water', *Water Science Technology*, vol. 55, no. 3, pp. 87 -96.

Scholz, M & Grabowiecki, P 2006, 'Review of Permeable Pavement Systems', *Building and Environment*, Vol. 42, pp. 3830 - 3836

Shi, J, Chen, S, Wang, S, Wu, P & Xu, G 2009, 'Favourable recycling photocatalyst TiO_2/CFA: Effects of loading method on the structural property photocatalytic activity', *Molecular Catalysts*, vol. 303, pp. 141 - 7.

Sonebi, M, Bassuoni, M 2013, 'Investigating the effect of mixture design parameters on pervious concrete by statistical modelling', *Construction Building Materials,* vol. 38, pp. 147 – 154

Takata, Y, Hidaka, S, Masuda, M, Ito, T 2003, 'Pool boiling on a superhydrophilic surface', *International Journal of Energy Research*, vol.27, pp.111-19

Taoda, H 2008, 'Development of TiO_2 photocatalysts suitable for practical use and their applications in environmental clean up', *Res. Chem. Intermed*, vol. 34, no. 4, pp. 417 -26.

Tong, B 2011, 'Clogging effects of Portland cement pervious concrete, Iowa State University, Graduate Thesis – 12048

United States of America, Environmental Protection Agency, 2007 'Method 8720D, Semivolatile Organic Compounds by Gas Chromatography/ Mass Spectrometry'

Wang, K, Schaefer, V, Kevern, J, & Suleiman, M 2006, 'Development of Mix Proportion for Functional and Durable pervious Concrete', *NRMCA Concrete Technology Forum*.

Zhuge, Y 2007, 'A review of permeable concrete and its application to pavements', *Taylor and Francis Group*, pp. 601-07, *Christchurch, New Zealand, 19th Australasian – Conference of the Mechanics of Structures and Materials.*

Zouaghi, A, Nakazawa, T, Imai, F, Shinnishi, N 1998, 'Permeability of no-fines concrete, Transactions of the Japan Concrete Institute', vol. 20, pp.31-38.

Appendix D Safety Issues

The research did not involve the following;

* Animals, nor tissue
* Human participants, nor issue
* Genetically modified organisms
* Biologically hazardous materials

The research involved handing of chemical materials.

Correct Personal Protection Equipment (PPE), will be worn when handing the following;

Table D.1 PPE Matrix

Product	***Hazard***	***PPE***
Cement	Skin, eyes, breathing	Safety glasses, eye protection, breathing mask
TiO_2	Skin eyes, breathing	Safety glasses, eye protection, breathing mask
PAH	Skin, breathing	Gloves, eye protection, fume hood
Epoxy Resin Part A	Irritation to eyes and skin	Gloves, eye protection, fume hood
Epoxy Resin Part B	Respiratory irritation, eyes, burns	Overalls, gloves, long sleeve shirt, fume hood, goggles
Manual Handling Samples	Lifting strain, crush injury	Correct lifting technique, equipment, correct storage
UV Light	Burns to eyes and skin	Safety UV glasses and full length clothing

Appendix E Research Timeline

The following research has been undertaken on a part time basis. A 12 month leave of absence was also taken in 2012.

Figure 4.1 Research timeline submitted with research proposal

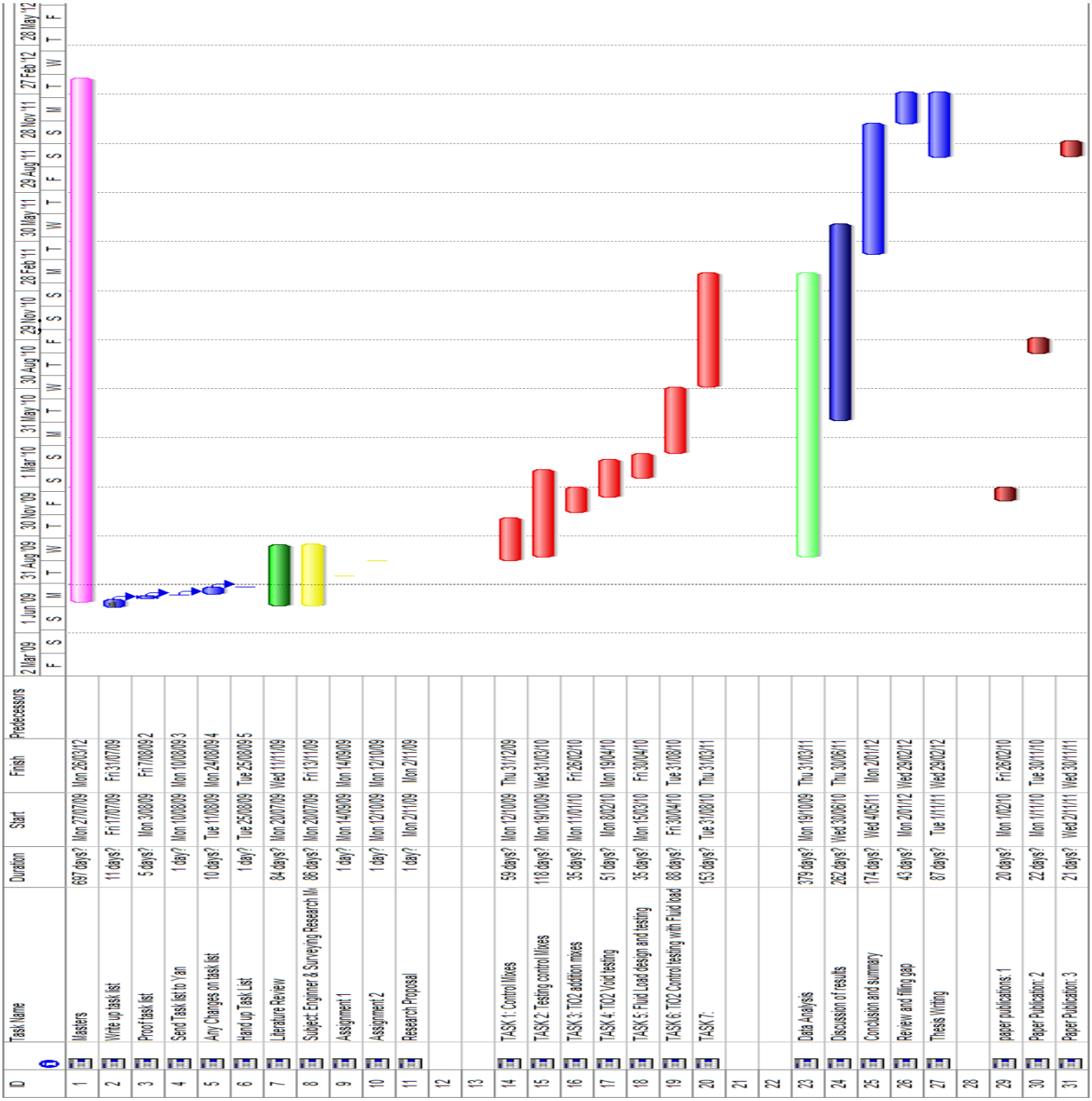

ID	Task Name	Duration	Start	Finish	Predecessors
1	Masters	697 days?	Mon 27/07/09	Mon 26/03/12	
2	Write up task list	11 days?	Fri 17/07/09	Fri 31/07/09	
3	Proof task list	5 days?	Mon 3/08/09	Fri 7/08/09	2
4	Send Task list to Yan	1 day?	Mon 10/08/09	Mon 10/08/09	3
5	Any Changes on task list	10 days?	Tue 11/08/09	Mon 24/08/09	4
6	Hand up Task List	1 day?	Tue 25/08/09	Tue 25/08/09	5
7	Literature Review	84 days?	Mon 20/07/09	Wed 11/11/09	
8	Subject: Engineer & Surveying Research Mi	86 days?	Mon 20/07/09	Fri 13/11/09	
9	Assignment 1	1 day?	Mon 14/09/09	Mon 14/09/09	
10	Assignment 2	1 day?	Mon 12/10/09	Mon 12/10/09	
11	Research Proposal	1 day?	Mon 2/11/09	Mon 2/11/09	
12					
13					
14	TASK 1: Control Mixes	59 days?	Mon 12/10/09	Thu 31/12/09	
15	TASK 2: Testing control Mixes	118 days?	Mon 19/10/09	Wed 31/03/10	
16	TASK 3: T0Q2 addition mixes	35 days?	Mon 1/10/10	Fri 26/02/10	
17	TASK 4: T0Q2 Void testing	51 days?	Mon 8/02/10	Mon 19/04/10	
18	TASK 5: Fluid Load design and testing	35 days?	Mon 15/03/10	Fri 30/04/10	
19	TASK 6: T0Q2 Control testing with Fluid load	88 days?	Fri 30/04/10	Tue 31/08/10	
20	TASK 7:	153 days?	Tue 31/08/10	Thu 31/03/11	
21					
22					
23	Data Analysis	379 days?	Mon 19/10/09	Thu 31/03/11	
24	Discussion of results	282 days?	Wed 30/06/10	Thu 30/06/11	
25	Conclusion and summary	174 days?	Wed 4/05/11	Mon 2/01/12	
26	Review and filling gap	43 days?	Mon 2/01/12	Wed 29/02/12	
27	Thesis Writing	87 days?	Tue 1/11/11	Wed 29/02/12	
28					
29	paper publications: 1	20 days?	Mon 1/02/10	Fri 26/02/10	
30	Paper Publication: 2	22 days?	Mon 1/11/10	Tue 30/11/10	
31	Paper Publication: 3	21 days?	Wed 2/11/11	Wed 30/11/11	